University of Stavanger

Faculty of Science and Technology

MASTER'S THESIS

Study programme/specialisation: Master of Science in Petroleum Engineering, Drilling and Well Engineering	Spring semester, 2018 Open
Author: Muhammed Mahmoud Abdelrhman Elsheikh	…… (signature of author)
Programme coordinator: Kjell Kåre Fjelde	
Thesis title: **Modelling and Simulation of Annular Pressure Build up**	
Credits (ECTS): 30	
Key words: AUSMV scheme, Drift flux model, Geometry expansion, Temperature driven, Matlab, Annular pressure buildup.	Number of Pages: 78 + supplemental materials/other: 19 Stavanger, June 15/ 2018

Abstract

Annular pressure buildup (APB) has been a concern for well design in the recent years. It is a phenomenon that relates mainly to subsea wells with possibly no means to release the pressure building up in closed annuli. Studying the factors, conditions, prediction methods and mitigation techniques are of immense importance to ensure secured drilling and production operations through the entire life of oil and gas wells. The main focus in this thesis is on temperature driven annular pressure build up that can take place in sealed annuli when production is initiated and warm productions fluids are brought to surface.

Modeling of the APB has been considered in the literature and it has been studied by researchers from different perspectives. An important aspect of this phenomenon is the influence of annular pressure buildup on changing the geometry of the annuli in an oil well. As the temperature in the annuli increases it will lead to a thermal expansion of the fluids which again leads to a pressure build up since the fluids will not be allowed to expand if the geometry is fixed. This pressure build up will in turn apply stresses on the surrounding tubing and casing strings that may exceed burst and collapse design limits and can eventually cause a severe failure or abandonment of the well in the worst scenario. However, the pressure build up will also change the geometry of the well. Changing the annular geometrical volumes will limit the pressure build up since some additional volume will be created allowing some real expansion of fluids during the temperature increase. Hence the pressure build up will not be as severe as the most conservative models predict.

Studying and modeling the effect of APB on the annular geometric change is the focal point of this thesis. Based on the drift flux model, a numerical scheme called the AUSMV (The Advection Upstream Splitting Method) is used to perform the simulations using the Matlab programming software. The scheme has proved to be a robust and reliable tool for solving one-dimensional, two-phase transient models. The main objective is to assess the ability of the AUSMV scheme to handle the geometry change of the A-annulus due to APB. A simple model has been used for the geometry changes as a starting point for future studies.

The annular geometrical changes have been modeled from different views. First a base case is considered where it shows the annular pressure buildup through time in absence of any geometrical changes. By doing that we can compare the performed simulations against the base case. The AUSMV scheme has shown its ability to handle the geometrical changes in the A-annulus in a robust manner and the simulations show different results whereas different annular fluids are used. Water based fluids are more sensitive to changes in annular volume than oil in relation to APB for the simple geometry model chosen. In addition, the bulk modulus (inverse compressibility) and thermal expansion coefficients are varied to investigate their influence on the pressure buildup of the trapped annular fluids. The results show that slight increase in the values of the bulk modulus or thermal expansion coefficient can increase both magnitude and rate of APB significantly. Another factor to be considered is the phase volume fractions of the mixture fluid which consist of liquid and barite phase. The results have proved that the rate of APB increases by decreasing barite concentration in the mixture.

A more sophisticated liquid density model where all annular fluid components are considered is recommended for future work in order to achieve more representative results rather than the simple fluid density model used in this thesis. As we have seen, the APB is very dependent of the compressibility and thermal property and this will change when considering a fluid mixture.

In addition, there is a room for more improvements to the AUSMV scheme to include other factors related to APB (e.g. barite settling) and a more sophisticated physical model for predicting the geometrical changes as pressure increases.

Dedication

To whom all belongs to, to the Almighty God whose no achievement is gained without

Acknowledgment

I gratefully thank my dedicated supervisor Kjell Kåre Fjelde for his patience, time and support. Without his astonishing notes and comments, this work could not be done.

Contents

List of Figures

List of Tables

Nomenclature

APB – Annular pressure Buildup

API – American Petroleum Institute

ASME – The American Society of Mechanical Engineers

AUSMV – Advection Upstream Splitting Method

BP – British Petroleum

CFL – Courant-Friedrichs-Lewy

HPHT – High Pressure, High Temperature

OBF – Oil-Based annular Fluid

PVT – Pressure-Volume-Temperature

TOC – Top of Cement

WBF – Water-Based annular Fluid

1 Introduction

In the recent years, well integrity has been a concern for the oil industry. It is defined by (NORSOK D-010) as the "*Application of technical, operational and organizational solutions to reduce risk of uncontrolled release of formation fluids throughout the life cycle of a well*". When production operations start, hot reservoir fluids flowing to surface contact the colder trapped fluids in the annuli. Consequently, heat transfers through tubing and casings resulting in thermal expansion and pressure buildup in the A, B and C annuli if these are sealed. This phenomenon may have severe effects and should be considered properly in subsea well design.

Annular pressure buildup

Annular pressure buildup is considered a serious issue with subsea drilling and production operations especially for HPHT wells. It takes place when fluids trapped in annuli are heated by the produced reservoir fluids. If a surface wellhead is used, annuli pressures can be relieved through casing valves and vented to surface facilities. However, in subsea completion releasing the annular pressure becomes a challenge. Eventually, disastrous consequences may occur and lead to loss of production.

Geometry change

APB caused by temperature increase can lead to geometrical changes to tubing or casing geometries if there is no possibility to release the excess pressure. The main objective of the thesis is to make the first steps in showing that the AUSMV scheme can handle geometry changes by using a simple model for the volume changes. However, the thesis tries to cover this objective from distinct aspects. These aspects include the type of annular fluid, barite

concentration in the fluid mixture and the influence of bulk modulus and thermal expansion coefficient of the liquid on the rate of APB.

The model used in this thesis can be regarded as a combination of the drift flux model and a numerical scheme called the AUSMV-scheme. A model previously being implemented in Matlab has been modified to include the simple model for the geometry changes. The code can be found in the Appendix. The drift flux model can describe one or two phase flow in pipes in one-dimension. It is transient and can be regarded as an example of nonlinear hyperbolic systems of partial differential equations. Based on the drift flux model, the AUSMV scheme was proposed by (Evje and Fjelde, 2002) which is the modeling tool used to perform simulations in this thesis.

Thesis structure

The second chapter of the thesis represents an overview about annular pressure buildup. It covers the definition of APB, the root causes, mechanisms and conditions that need to be present for building up the annular pressure. The chapter also expresses the basic theory of APB mathematically and the major consequences that such phenomenon may cause to the well, environment and personnel. The chapter ends with a summary of common mitigation techniques used by the industry in order to predict and suppress the effect of APB.

The need and importance of modeling APB and the associated geometry changes are presented in the third chapter. A theoretical overview about two fluids flow in pipes is covered as well. In addition, a literature review of models of heat transfer in oil wells is highlighted as heat transfer plays a significant role for thermal expansion of annular fluids. The chapter also reviews some of the main contributions made by scholars in the field to model geometry changes in oil wells due to APB and the models they provided to understand more this issue.

The fourth chapter explains in more details the concept and theory behind the transient drift flux model and how it is used to perform simulations for this kind of studies. The numerical

AUSMV scheme basic concept which is based on the drift flux model is deliberated as well. The AUSMV scheme is modified in Matlab to fit the purpose of this thesis. Other related topics to the scheme are highlighted as well such as discretization, slope limiters and CFL condition. Furthermore, some of the models for calculating fluid temperature around the wellbore are discussed at the end of the chapter.

The fifth chapter of this thesis includes results and discussion of the simulations done and their input parameters. The results are divided into several sections including a base case of APB without volume expansion, simulations of water and oil based annular fluids with area change, simulation results when the density model parameters are varied, a comparison between oil and water based annular fluids and finally what may happen if we modify barite concentration in the fluid mixture and the resultant effect on the APB.

In the final chapter, a brief conclusion and thesis findings are discussed, in addition to what can be recommended for any future work on this topic.

2 Annular Pressure Buildup

2.1 Background

Annular pressure build up can be caused by different mechanisms like for instance hydrocarbon leakages. Here we will focus on temperature driven annular pressure build up that can take place in closed annuli when production is initiated and warm production fluids are brought to surface. The upper part of the well will warm up and the fluids in the annuli will try to expand. However, since the annuli are closed, this will instead lead to a pressure build up.

In most onshore, platforms and shallow water wells, associated annular pressure can be relieved by opening casing valve and venting the pressure to surface facilities to a tank or a flowline, whereas it is widespread practice to overlap a previous casing shoe with cement (Gate energy, 2015) . Accordingly, the annulus above becomes sealed as presented in **Figure 2.1**. Nevertheless, subsea wellheads used in deepwater wells normally do not have access to the outer annuli in the well. However, in some cases only the tubing that provide access to the production casing annulus, known as the A-annulus, may be monitored and hence any associated pressure can be bled down (Williamson et al., 2003). During well construction and production operations, the capacity of the well to withstand pressure variations should be considered in well design. In addition, it is beneficial to consider calculations of potential pressure changes to determine how severe the issue can be and predict proper mitigation techniques. Furthermore, casing design should reflect the mitigation strategy of the APB.

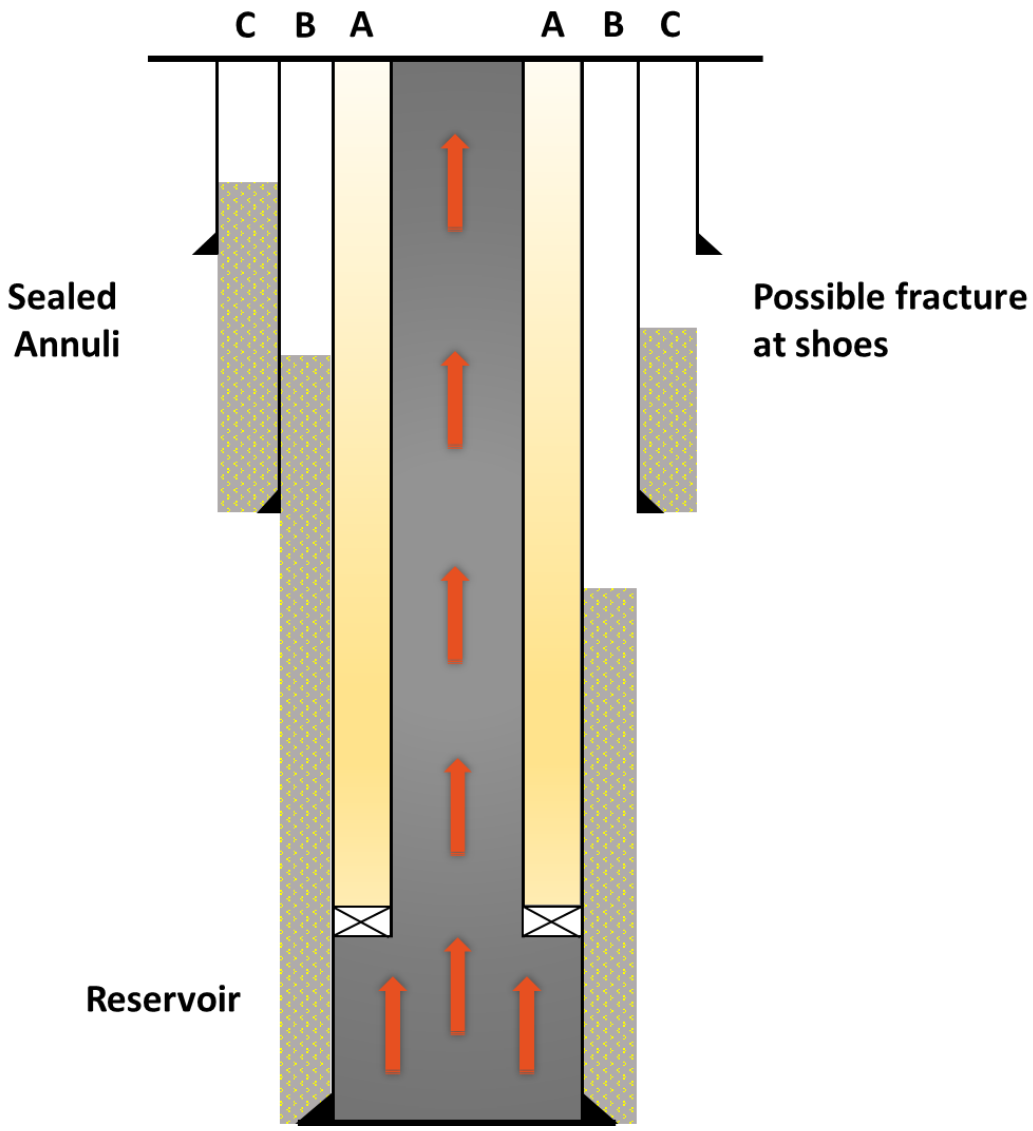

Figure 2.1 Typical casing program and wellbore under production.

2.2 Concept and Mechanism behind APB

The Concept of APB

After completion or long production stop, the well itself will have a temperature that is the same as the geothermal temperature determined by the geothermal gradient. However,

during production startup, warm hydrocarbon fluids will be brought from the deep reservoir up to surface through the production tubing which in turn heat the shallower parts of the well (Moe and Erpelding, 2000). **Figure 2.2** illustrates the annular temperature before and after production.

As a consequence, the trapped fluids in the annular will try to expand but since the expansion is restricted, the pressure has to increase if the temperature increased. This is easily seen from the formula Mass = density(p,T) x Volume. Mass is conserved, and if volume is unchanged, density must be unchanged. So if the temperature increases, the density will tend to reduce and this must be compensated by an increase in pressure to maintain the density value constant. However, one shall have in mind that the annuli might allow some volume expansion when the pressure increases due to the elasticity of e.g. steel used in production tubing and casings.

In consideration of the incompressible nature of these fluids, slight changes in parameters such as temperature or annular volume may lead to significant changes in pressure in fully isolated annuli (Oudeman and Bacarreza, 1995). In the extreme cases, pressure may develop high enough leading to collapse the casing and forcing the well to be abandoned. Annular pressure buildup has an excessive effect on casing strings by applying excessive loads, that is why it has to be considered properly in the design phase in order to assure well integrity throughout well productive life (Alcofra et al., 2014).

Wells which are drilled in deepwater are likely to be vulnerable to annular pressure buildup because of the cold seabed temperature at installation, in opposition to elevated subsea wellhead temperatures during production (Williamson et al., 2003). Such wells are susceptible to large temperature increase while the initial temperature at installation can be as low as the sea temperature. However, high reservoir temperature is common in many deepwater wells and these wells are probable to produce at very high flow rates which in turn can bring bottomhole static temperature to near the mudline (API RP 96 2013).

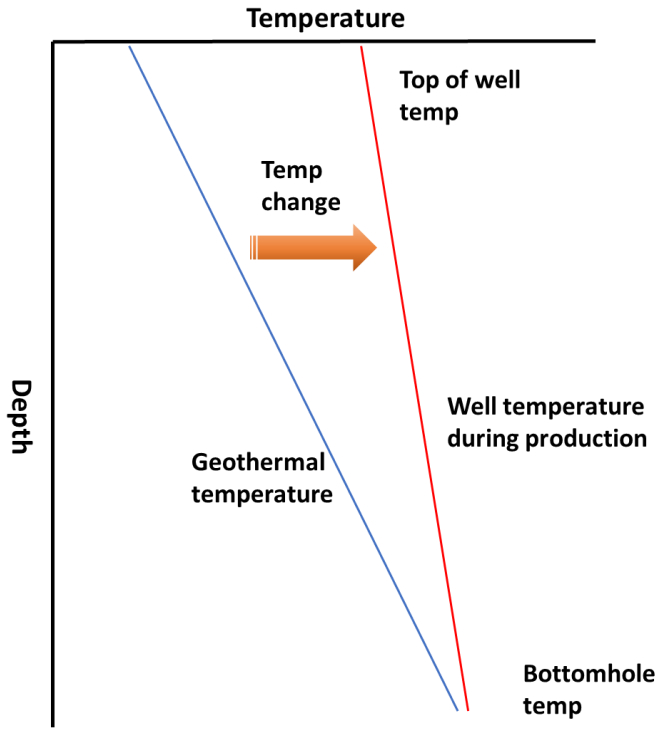

Figure 2.2 A simplified temperature profile before and after production, the arrow indicates the increase in temperature due to oil production.

To simplify the concept of annular pressure buildup it is beneficial to consider the illustration in **Figure 2.3**, which shows a typical wellbore configuration similar to **Figure 2.1** but seen from above. The A-annulus is the space between the tubing and the 9 5/8 in production casing while B-annulus represents the space between the production casing and the 13 3/8 in intermediate casing. The outermost annulus is the C-annulus in this case. During production, reservoir fluids flow to surface in elevated temperature. Heat will be transported to surface by convection (transport of fluids). Consequently, production tubing, casings and annuli fluids heat up. The fluids in the annuli will heat up both due to conduction and convection. The first is due to radial heat transfer from the tubing and outwards while the latter will be due to a redistribution of fluids inside the closed annuli due to temperature differences vs depth (Ettehadi et al., 2014). In turn, the fluids filling these annuli will try to expand.

If an annulus is sealed up with cement or if settled weighting material as barite makes a barrier and leading to a closed annulus, then the annular pressure will build up (API RP 96 2013). If the annulus is closed, the generated pressure will be dependent on how much the fluid is heated besides the thermophysical properties of the suspension (Udegbunam et al., 2017) and the rheological properties (Ettehadi et al., 2014). Rheological properties include annular fluid viscosity, weight density, solid volume fraction, consistency index, etc. Enhancing such parameters can lead to reducing the sedimentation of annular fluids and hence minimizing the convective flow of heat. In addition, it will also depend on eventual expansion of the annuli due to pressure differential increases.

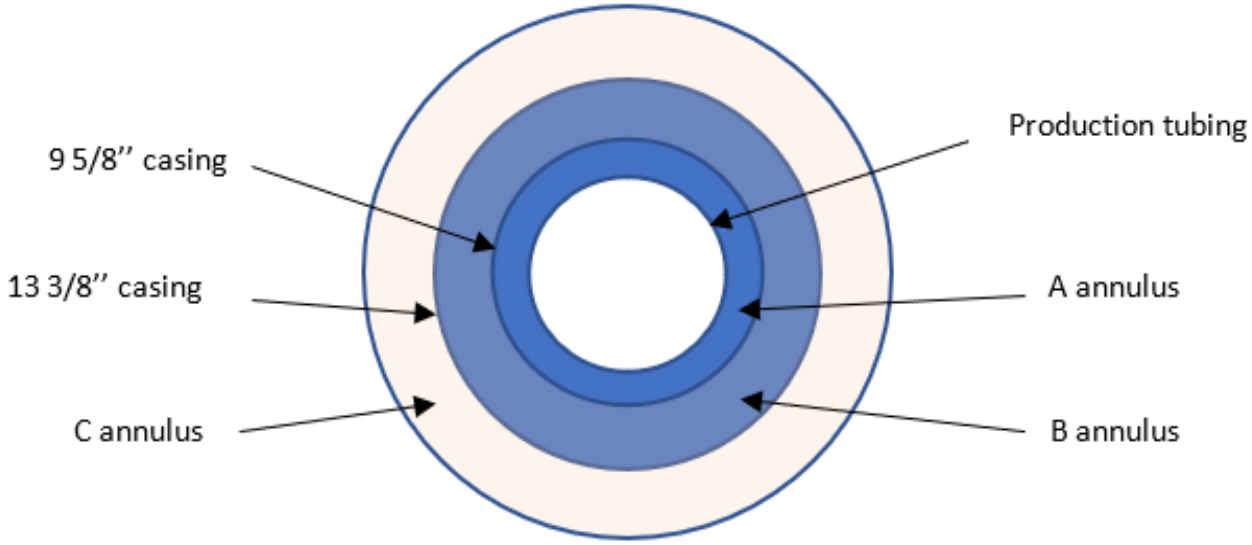

Figure 2.3 A horizontal view of wellbore configuration with different annuli.

Annular pressure build up depends on two separate effects. First, it depends on how much the fluid will try to expand. Secondly, it will depend on how much it is allowed to expand due to geometry changes caused by tubing and casings displacements. The increase in pressure will change the volume of the annular space due to the elasticity of the steel. Both effects will

have impact on what the final pressure build up will be and they are working in different directions. The attempt for the fluid to expand due to temperature increase in a confined space will increase pressure but some relief might be seen if the annular volumes are increased.

When a well experiences a temperature driven annular pressure buildup, two conditions have to be present (Vargo Jr et al., 2003; Williamson et al., 2003). The first condition, a sealed annulus must exist and secondly a temperature increase must occur. Normally, when a formation is drilled, it will be isolated by casing, then a cement slurry is circulated up on the outside of the casing, and the top of cement (TOC) is often set inside the annulus of the previous casing. Once the wellhead is sealed, an isolated volume is created or trapped, and this is why it is called 'trapped fluid'. When the trapped fluid is heated by drilling and production operations, it will expand and may result in a considerable pressure growth. Such pressure increase can be compounded if more than one annulus is sealed (Williamson et al., 2003).

Barite Sag

The phenomenon of settlement of weighting-material elements in drilling fluid is known as barite sag, which can potentially impose significant operational issues for drilling, including lost circulation, well-control difficulties, poor cementing operation, and stuck pipe (Adariani, 2012). Settlement of the weighting materials is widely known as barite sag since barite is the most popular weighting material used in drilling industry.

When completing the well, the annular spaces between casings are filled with clear drilling fluid while the annular space between the tubing and production casing is filled with a completion fluid (Ettehadi et al., 2014). These fluids (especially in the outer annuli) can have weighting material particles that may settle over a longer time period depending on their rheological properties and thermal conductivity.

The settling of solid particles affects the thermal properties of the drilling fluid and hence the annular pressure increases. Due to sedimentation the annular fluid settles into a clear fluid and slurry of weighting elements and hence have different thermal conductivity and heat capacity compared to a fluid mixture which in turn affects the APB (Ettehadi et al., 2014). In addition, the temperature change in the annuli will be larger on top than bottom so the location and length of the clear liquid zone will also have impact. However, in order to eliminate issues related to barite sag, the impact of different drilling parameters on barite settlement and sag phenomenon should be well understood in consort with mathematical formulation and modeling of settlement and sag processes (Movahedi et al., 2018).

Other mechanisms for APB

Convective and conductive heat transfer through fluids trapped in the annuli between casing strings is a major driving force for building up annular pressure (Ettehadi et al., 2014). However, in addition to thermal effects described previously, annular pressure change may be due to other means (API RP 96 2013) and can be driven by:

- Downhole gas lift operations for production optimization (i.e. gas lift via A-annulus).
- Pressure leakage via completion components such as production packers.
- Pressure leakage through casing or production tubing.
- Leakage along the crossover valves in subsea tree.
- Leakage from an HP or LP hydraulic line.
- Leakage from a downhole chemical injection line.
- Wellhead or tubing hanger leakage.

Proper well design

Well design must ensure that stresses related to production of hydrocarbons do not compromise the integrity of the well during drilling and completion operations. The selected

casing to be run in the wellbore must be able to resist all loads that may take place throughout the well life. This will also include the load scenario caused by APB which for instance takes place during production startup. In case that the estimated annular pressure build-up exceeds casing limit, suitable mitigation strategy or management technique should be considered to prevent the possibility of casing failure (Alcofra et al., 2014). Real cases of casing collapse reported in some wells in the Gulf of Mexico due to APB, indicating the seriousness of the subject. (Bradford et al., 2002; Vargo Jr et al., 2003) showed how BP plc experienced a well failure in the Marlin development in Deepwater Gulf of Mexico, where within only few hours of production startup, the production tieback casing collapsed, leading to failure of the production tubing. After thorough investigation, the most likely cause of the failure was identified to be pressurization of the outer annuli due to production thermal effects.

2.3 APB Fundamental Theory

The basic theory

According to (Aadnøy, 2011; Moe and Erpelding, 2000), the fundamental theory for annular pressure buildup from thermal effects can be explained numerically in a straightforward way as follows:

When unconstrained fluid filling an annulus is heated, it will expand to a larger volume which is defined by the following Equation:

$$V = Vo\ (1 + \alpha \Delta T) \tag{1}$$

Where: $V =$ Expanded volume, in^3.

$Vo =$ Initial volume, in^3.

$\alpha =$ fluid thermal expansion factor, R^{-1}.

$\Delta T =$ Average fluid temp. change, °F.

While if we consider a constrained fluid by a perfectly rigid container, the increase in pressure is calculated as shown in Equation 2 as follows:

$$\Delta P = (V - Vo) \, / VoBn \tag{2}$$

Where: $\Delta P =$ Fluid pressure change, psi.

$Bn =$ Fluid compressibility, psi^{-1}.

By substituting Equation 1 into Equation 2, the result is Equation 3 which shows the pressure increase as a function of the fluid properties and the average temperature change for a simple case of fluid expanding inside a rigid container:

$$\Delta P = \alpha \Delta T / Bn \tag{3}$$

Geometrical changes

Fortunately, tubing and casing strings are ductile and not brittle containers; thus they are able to expand or shrink to some extent. With pressure increase, the inner and outer strings

containing the fluid move slightly where the inner string gets a smaller diameter and the outer string gets a larger diameter. This leads to an increase in the contained volume and therefore the well experiences a reduction in the pressure build up as a consequence. Additionally, wellhead growth may take place due to thermal increase of the tubulars and in the same manner this leads the contained volume to expand and hence to reduction in the associated pressure (Moe and Erpelding, 2000).

2.4 Consequences of temperature driven APB

It was mentioned previously that wellheads used in onshore and platform wells are readily accessible, which allow the operator to monitor and bleed off any annulus through surface facilities when needed. Yet, this is not the case when using subsea wellheads in exploration drilling, where there is no venting capabilities to the annulus between the tubing and the production casing (Aadnøy, 2011). Access to such wellhead is largely limited and needs attentive consideration of annular pressure increases during casing design phase.

Every annulus in any well is subject to annular pressure buildup as long as that annulus is full of fluid, which is the case in most annuli. However, the threat of damage during production can be defused by bleeding of the fluid pressure given that there is a surface access to the annulus. Alternatively, the pressure buildup can be avoided if there is an access to a permeable formation which might act as a natural valve to limit the buildup allowing the expanded fluid to escape through (Jandhyala and Chiney, 2014), as seen earlier in **Figure 2.1**.

Not only during production

Furthermore, annular pressure buildup is not a phenomenon that related only to production, but also it may occur throughout testing and drilling operations (Perdana and Zulkhifly,

2015). The industry has reported cases where APB was determined to be the cause of well failure during drill-ahead operations (Pattillo et al., 2004). In addition, subsea high-pressure and high-temperature (HPHT) wells can be subjected to large casing heat-up during drilling or testing where tubulars elongate and annuli trapped fluids expand; resulting in severe loads that have to be considered extensively during casing design (Mitchell and Wedelich III, 1989). Such loads may lead to well failure in terms of burst and collapse in the tubulars, but they are not the only concern. (Halal and Mitchell, 1994) emphasized the role of axial loads and stated that ''*Casing axial loads from constrained thermal elongation together with "reverse ballooning" from high annular pressure can generate sufficient compression to relieve all hanging weight and cause upward forces at the mudline hanger*''.

Severe damage

The consequences of APB would be catastrophic and harmful in the absence of bleed off or formation fracture, leading to loss of production (Vargo Jr et al., 2003) or to loss of the well in the worst case. The manifestation of such buildup would be in one or more ways and according to (Moe and Erpelding, 2000) the followings examples show what might arise in such cases:

1. The A-annulus can build up enough pressure inducing radial, axial and hoop stresses on the production tubing and production casing surfaces leading eventually to collapse of the production tubing or rupture (burst) of the production casing (9 5/8 in). **Figure 2.4** represents an illustration of what a collapsed casing may looks like.

2. An extensive heat up may take place in the B-annulus between the production casing and the protective casing (e.g. intermediate casing 13 3/8 in). Such thermal expansion may reach to a point where the production casing collapses or the protective one bursts. The same can happen in the C-annulus as well.

In general, the inner strings are more vulnerable and more susceptible to failure comparing to outer casings (Moe and Erpelding, 2000). This is due to the fact that heat disperses as it spreads out to the larger strings. Unfortunately, even expensive and high-grade production strings are often designed with too low design factor causing such catastrophic consequences.

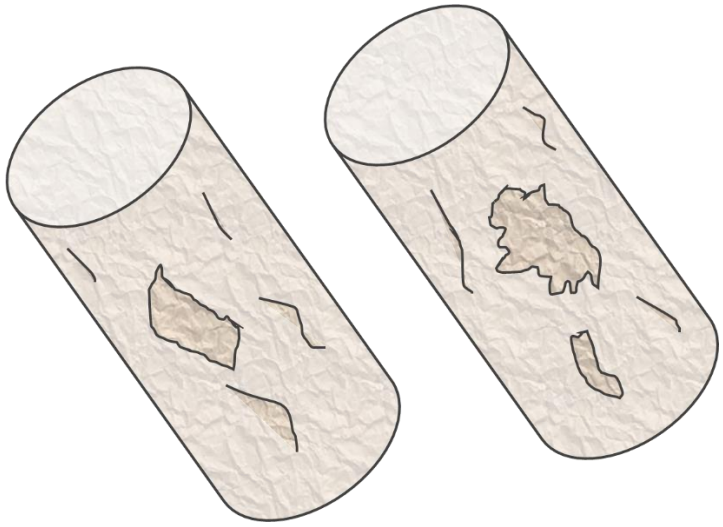

Figure 2.4 A schematic illustration of collapsed casings.

2.5 APB Mitigation Techniques

Throughout the years, the industry has reported several cases of APB causing casing collapse and failure of production tubing (Sathuvalli et al., 2016), where some examples have been stated earlier in this chapter. Several methods have been used to mitigate the effect of APB. It is useful to recall the two conditions that must exist such that APB phenomenon can present, as most of the mitigation practices count on those conditions. The conditions are a

sealed annulus and temperature increase. The sealed annulus is associated with cementing operations. When the well is isolated and the top of cement (TOC) is set inside the previous casing, a trapped volume of liquid is created. Therefore, a temperature increase occurs due to drilling and production operations. As a result, the trapped fluid expands producing a substantial pressure increase.

Both operational techniques and completion equipment solutions are implemented and can be incorporated into drilling and completion programs to mitigate the APB. (Williamson et al., 2003) listed some of the common existing solutions as the following: cement shortfall, full height cementing, leak path, crushable foam wrap, absorb volume fluids and enhanced casing design. Some of these solutions eliminate the APB failure while others mitigate the effect.

Common mitigation methods

- **Cement shortfall**

This solution aims to ensure flow paths and prevent the first condition, "sealed annulus", to occur (Aadnøy et al., 2009). Setting the Top of Cement (TOC) below the previous casing shoe allows fluids to escape to the formation and prevent trapping. Extra measures must be considered before designing shortfall cement. Characteristics such as mud displacement and settling of mud weighting materials need to be well studied to ensure the success of this method. Poor mud displacement can result in setting the TOC above the previous casing shoe with a sealed annulus as a result. On the other hand, the settling of mud weighting materials such as barite might cause a trapped condition and resulting in APB failure (Williamson et al., 2003).

- **Full height cementing**

This solution aims to prevent the first condition "sealed annulus" by filling the annulus with cement. However, this solution might cost a lot and take time.

- **Preferred Leak path or bleed port**

Leak path is a completion design related method and also known as burst-disk technology. This technology mitigates the effect of APB by allowing the casing to fail outward in a predictable manner and give venting path to fluids to pass out. This method has been tested extensively and performed well. However, some operators are trying to investigate more appropriate means as they think a controllable failure is not acceptable (Williamson et al., 2003).

- **Syntactic crushable foam wrap**

syntactic foam is manufactured to collapse at a specific pressure and installed on the external casing wall. It is regarded as an cost effective solution to mitigate APB and protect casing strings in offshore HP/HT wells (Liu et al., 2016). Syntactic foam is a class of material created by filling a polymer, metal, or ceramic matrix with hollow glass microspheres. Adding (2 - 8% of the trapped volume) crushable foam wrap to annulus prevents pressure build up expansion (Williamson et al., 2003).

- **Absorb volume fluids**

This method assumes that fluid is sealed and aims to absorb the volume build up in annulus by injecting compressible fluids in the trapped annulus. 5% of the annulus volume is placed at the top of the annulus (Williamson et al., 2003). The contraction of Nitrogen when pressure builds up can be used to absorb enough volume preventing casing failure.

- **Enhanced casing design**

This method aims to prevent casing failure as a result of APB by increasing the casing capability to accommodate higher pressure build up. Although this method seems to be more effective, it can be expensive and requires extensive studies to predict maximum pressures and best casing selection (Williamson et al., 2003).

- **Vacuum-insulated tubing (VIT)**

Thermal insulation has been used widely to mitigate damaging effects of annular pressure buildup (APB). Vacuum-insulated tubing consists of an inner and outer tube welded together at both ends where the annular space is evacuated and plug welded. VIT is considered one of the viable technologies used in mitigating APB effects (Azzola et al., 2007).

3 Modeling of APB and Geometry Expansion

The development of a program for thermal analysis of oil production wells requires a flow model that can describe the heat transport in the production tubing and the heat transfer from the tubing to the surrounding annuli. This leads us to consider models that include conservation of mass, momentum and energy. Usually, the fluid element receives heat through fluid convection mechanism while losing heat to the surroundings via conduction (Hasan and Kabir, 2012). This heat flow is a function of the heat transfer mechanism observed, the properties of the medium in which it propagates and the difference between the temperatures of the fluid and the formation. Furthermore, for the calculation of APB, it is necessary to define the properties of the fluids of the annular, initial conditions of the well and structural properties of the well that will allow annular volume change or casing deformation. In order to introduce the subject properly, initially a summary of the evolution of modeling of wells is presented. Subsequently, a heat transfer overview will be expressed, and eventually, the proposed models and their main contributions will be presented.

3.1 Why to model APB

The temperature difference between hot production fluids and trapped fluids in the sealed annuli is considered as the main reason for annular pressure buildup. The consequence would be a pressure increase that might be quite high because of the annulus fluid low compressibility. Thus, the well integrity and casing safety are put in danger, especially in the high pressure high temperature (HPHT) subsea wells.

Continual demand for oil and gas increases the desire to search for new reservoirs, challenging the industry and pushing it to look for oil and gas in harsh environments where high pressure and high temperature (HPHT) wells need to be drilled (Barcelos et al., 2017). Such types of wells require a great amount of caution and special tools or equipment to be

able to monitor their conditions. There is also an endless risk of failure which can be due to loss of productivity, leaks or even undesired total loss of the well (Azzola et al., 2007; Oudeman and Kerem, 2006).

Annular Pressure Buildup is an important phenomenon in the field of well integrity, which was described previously as the pressure increase due to thermal expansion of the trapped fluid within the annulus caused by the upward flowing of hot reservoir fluids. APB is considered one of the main probable problems that may take place during well construction and production because of its ability to leave terrible consequences to the integrity of the well (Bradford et al., 2002). Although there are many strategies and mitigation techniques that have been developed to mitigate APB, still there is a lack of robust models that can predict to decent accuracy the complex heat transfer or the petroleum production multiphase flow process in order to give support to well design and construction (Barcelos et al., 2017).

The precise prediction of the pressure and temperature along the tubing string and in the annuli is quite important in well design. According to (Barcelos et al., 2017), the importance arises as such prediction is critical for:

(i) Decision making on flow assurance strategies,
(ii) Corrosion calculations and erosion rates,
(iii) Identification of potential risks related to pressure buildup.

3.2 Fluid Flows in Oil Wells

The most simplified model of well flow is single-phase flow. It can be used if there is produced oil without gas dissolved. Conservation laws of mass, momentum and energy are being widely used to solve fluid flow through pipes in steady state conditions. The mass rate in this case is constant at all positions in the tubing, although the densities and flowrates will change due to fluid expansion when fluids are transported towards the surface. However,

the flow can also be transient for instance due to time varying temperature conditions or due to time variations in the flowing rates.

However variations in the fluid properties and flow conditions can lead to phase change as the pressure falls. Here the need of an adequate two-phase flow model arises in order to include the gaseous phase of the mixture.

3.2.1 Two Fluids Model

Each phase in two-fluid model is considered individually (Bendiksen et al., 1991), while interphasial terms are used to compute the transferred mass, momentum, and energy between the phases. In addition, closure models are required as well for solving the unknowns in these terms.

According to (Bendiksen et al., 1991), when the continuity equations of a physical quantity for both phases are combined, the interphasial terms are eliminated, generating a set of equations for the mixture. This model is often referred to as the drift flux model and a transient formulation of that is for example shown in (Pauchon and Dhulesia, 1994). However, closing relations for pressure drop by friction and for phases volume fractions are required. The last relation can often be given indirectly by providing a gas slip relation expressing how gas moves in relation to the mixture flow.

3.2.2 Flow patterns in vertical and inclined pipes

Flow pattern models are generally derived from observation of two-phase flow and consideration of specific relationships for the friction pressure gradient and flow properties. Thus, it is necessary to define transition areas between models, in addition to relations between different phases properties. Each flow pattern shows specific features in relation to

void distribution, pressure gradients due to friction and gravity and other features for example those related to droplet drag.

Several flow pattern classifications are defined by scholars in the field, however, (Hewitt and Hall-Taylor, 1970) flow pattern classification is selected here as example for elaboration while **Figure 3.1** shows some of the main flow patterns in this definition. The bubbly, slug, churn and annular patterns are also present in the works of (Taitel et al., 1980; Wallis, 1969) among others. A brief description of each flow pattern is demonstrated in the following.

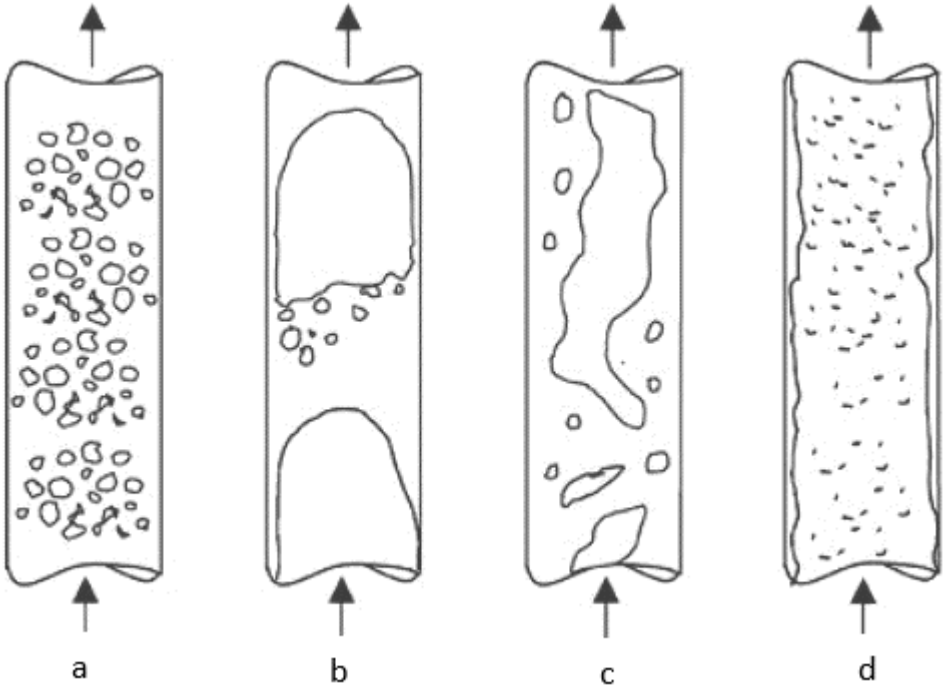

Figure 3.1 Flow patterns in vertical pipes a) bubbly, b) slug, c) churn and d) annular (Wallis, 1969).

Bubbly flow

Bubbly flow is characterized by the presence of gas bubbles of small diameters dispersed randomly in a continuous liquid phase. Furthermore, little relative motion between the phases takes place if the bubbles are distributed in a uniform way. This flow characterized

by complex interactions between the interfaces of bubbles and between the bubbles and the liquid flow as well.

Slug flow

As the gas volume increases and the coalescing of the bubbles gets intense, there will be a consequent increase in the void fraction resulting in larger bubbles followed by liquid slugs. These bubbles are bullet shaped, with a spherical nose and cylindrical tail with distortions. This flow characterizes the slug pattern, where in the center of the tube is the Taylor bubble occupying most of the flow, followed by the slug of liquid while in the region next to the wall a film of falling liquid appears. The liquid slug below the Taylor bubble may contain small gas bubbles, characterizing an aerated slug.

With the increase of the void fraction caused by the presence and the elongation of the bubble, the Taylor bubbles experience elongation and line up quite closely with the tail of the previous bubble touching the nose of the downstream bubble (Zhu, 2003). In this case, the liquid slug between the bubbles gets unstable and in addition it cannot sustain its shape because of the strong wake behind the bubbles.

Churn flow

Churn flow is to some extent similar to slug flow, but much more chaotic, foamy and highly disordered. The bullet-shaped Taylor bubble becomes narrower and distorted as a result of increasing the air flow rate for slug flow. The gas slugs are relatively unstable, and take on large, elongated shapes. However, the continuity of the liquid in the slug between successive Taylor bubbles is destroyed over and over again by a high local gas concentration in the slug (Zhu, 2003). As this takes place, the liquid slug falls, and the liquid accumulates forming a bridge, which is again lifted by the gas.

Annular flow

When the center of the flow has a continuous gaseous phase and the film of liquid on the wall becomes ascending upward, the flow is said to be annular. The gas flowing in the main stream can draw liquid droplets from the film which are charged by gaseous core in the form of captured droplets, and after that return to the film in the wall of the tube in a region downstream of the flow.

So, when trying to model production in wells and transport in pipelines one must model the PVT behavior of the hydrocarbon fluid, e.g. transition from one phase flow (oil with dissolved gas) to two phase flow (where free gas is present). But one must also be able to model the complex flow patterns occurring when we obtain a two phase flow system. The modelling can be complicated further when considering production of water in addition, leading to multiphase flow systems.

3.3 Heat Transfer in Petroleum Wells

For many years, several researchers worldwide have studied the heat transfer process while producing from oil and gas wells since the first key contribution by (Ramey Jr, 1962). Moreover, a reference work regarding the topic is reported by (Hasan et al., 2002). The model of (Ramey Jr, 1962), has been known as one of the pioneers in the field of modeling heat transfer in oil wells, consists of a model for the internal flow in a pipe, where the heat transfer in the fluid is considered steady state and the heat exchange with the rock formation is transient. However, the model is not designed for two-phase flow considerations but it was the base for later models defined by (Alves et al., 1992; Hasan and Kabir, 2012). Nevertheless, more recent models take into consideration the various physical properties of flowing fluids and two-phase flow scenarios in addition to other effects.

The model of (Alves et al., 1992) was developed on solving the fluid energy, where the temperature profile was assumed to function linearly with depth. Black Oil model was

applied in modeling the rigorous thermodynamic behavior of the flowing fluid. Moreover, water was solved explicitly with no count for the mass transfer between the phases. Therefore, according to the conditions imposed, the model can be reduced either to the Coulter and Bardon method or to the model previously presented by (Ramey Jr, 1962).

The model of (Hasan and Kabir, 2012) was developed for analyzing heat transfer on the outside of tubes. It proposes that heat transfers from the well to the surrounding formation via transient conduction where the flow is the source of heat. However, in the intermediate layers of well completion (e.g. the different annuli), the resistance of the various layers surrounding the production column is considered.

Generally, heat transfer can take various forms which involve thermal conduction, natural convection, thermal radiation or a combination of them. Moreover, heat transfer in the annulus depends mainly on the annular size and the materials filling the space (Zhou and Zheng, 2015). As the well depth increases, more technological issues come across in exploration, drilling, production or injection wells. Such issues arise due to the high-temperature and pressure, and deep geological conditions. However, wellbore production fluid continues to lose heat to the less warm surroundings through its journey upward along the borehole over long distance (Hasan et al., 2002). An example was presented by (Kanev et al., 1997) where numerical investigations were conducted to study the effect of heat loss from the geothermal wellbore on the temperatures and pressures of produced fluid. In their study, flow rate was regarded as a key parameter in shaping the wellhead conditions while geothermal gradient and elapsed time have smaller effects. They gave a description of a 3382 m deep geothermal well after 100 days of production by which the fluid temperature decreased from 301 °C at the bottom up to about 255 °C at the wellhead at mass flow of 150 t/h**.** A higher flowrate will bring warmer fluids faster to surface - by convection - and is therefore a very important parameter for what kind of temperatures that will be achieved at the wellhead.

3.4 APB Modeling

Annulus pressure formed between casing strings can be estimated by discretization of wellbore temperature. However, annular pressure buildup (APB) is considered by the mathematical models through:

(i) the trapped fluid expansion due to thermal expansion during production,
(ii) the deformation of surrounding formation and along casing walls,
(iii) leakages from wellbore to formation or at the well head.

These three contributions are presented in the equation proposed by (Oudeman and Bacarreza, 1995) and emphasized later by (Oudeman and Kerem, 2006) to calculate the pressure increase in the annulus as follow:

$$\Delta p = \frac{\alpha_l}{\kappa_T} \cdot \Delta T - \frac{1}{\kappa_T \cdot V_{\text{ann}}} \cdot \Delta V_{\text{ann}} + \frac{1}{\kappa_T \cdot V_l} \cdot \Delta V_l \qquad (5)$$

where:

κ_T is the coefficient of isothermal compressibility

α_l is the coefficient of thermal expansion

V_{ann} is the annular volume

V_l is the volume of annular liquid

ΔT is the increase of temperature

However, according to (Hasan et al., 2010), the first term is the dominant, contributing to almost 80% of the total pressure increase where it represents thermal expansion of the fluid. The negative sign in the second term implies that increasing the annular volume will lead to decreasing the APB and vice versa. The other two terms represent annular volume change and liquid leakage to seabed or surrounded formation. These terms give negative pressure and if ignored in the previous Equation, an overestimation of annular pressure buildup should be expected.

On the other hand, (Barcelos et al., 2017) focused on the estimation of APB using a robust two-phase flow and heat transfer model of the well. In their study, a 4700-m deep pre-salt production well composed by three concentric annuli were used in modeling. The model solution was made from bottom hole to wellhead, where each new axial position of the wellbore was computed based on the previous position gradient. Modeling of radial heat transfer was obtained via thermal resistance network approach and the annular pressure buildup was estimated using a new model, based on the analytical equation proposed by (Oudeman and Kerem, 2006).

3.5 Models of geometry changes

It has been mentioned in the previous chapter that two separate effects are responsible of Annular Pressure Build-up: the volumetric expansion of the trapped annular fluid and casing displacement. There is a coupling between these two effects in which they occur simultaneously as the casing determines the annular space. Moreover, if any element of the well experiences an expansion; this would influence deformation of all other elements. Models to calculate fluid volumetric variation have been a concern of several studies in the field (Adams, 1991; Ellis et al., 2002; Halal and Mitchell, 1994; MacEachran and Adams, 1991). However, (Halal and Mitchell, 1994; MacEachran and Adams, 1991) introduced some methods to analyze the deformations of multiple casings.

(MacEachran and Adams, 1991) emphasized the need for multistring analysis rather than the existing single-string models. In their paper they expressed that when the analyzed string is independent of others in the system (e.g., the tubing in a subsea well), the single-string analysis is adequate. However, when the stress in one string have an impact on the stresses in other strings in the system which means the strings behaviors are interdependent; a multistring analysis is required. The authors have demonstrated that it is not possible to calculate heat-up pressures at all using true single-string models because - by definition - they do not include data about other casings except the one under consideration. However, by introducing simplifying assumptions of the outer-string behavior, more advanced single-string models can overcome such limitation to some degree.

(Halal and Mitchell, 1994) went in the same direction by criticizing the conventional single string models and highlighting the need for a multistring approach. They claimed that as multistring effects are neglected, such type of models can underpredict or overpredict pressures between strings. In addition, using single-string analysis methods to assess heat-up pressure give results that are - in most cases - too high due to the common assumption that the casing of interest is surrounded by fully rigid structure. However, in their paper they used PVT relations for annular fluids and a composite elasticity for cemented casings in order to come up with a constitutive-based multistring analysis.

They presented a multistring analysis method that take into account three important effects: a composite stiffness of casings, cement, and formation; the relation between heatup pressures and axial stresses; and the non-linearity of fluid behavior as a function of pressure, temperature and composition. According to them, a 30% higher estimation of the annular pressures can result due to using a rigid single string well model. However, in contrast, if the well is considered as a fully flexible layer, the estimated pressures will also be in the range of 28% lower than the observed actual values.

Three categories characterized (Halal and Mitchell, 1994) modeling of trapped annular pressure and its relation to casing design: a wellbore thermal model, Annular Fluid Expansion model and casing-tubing displacement model. Several subsequent models were based on the previous study such as the work of (Alcofra et al., 2014).

On the other hand, a multistring model for multiple casing annuli was used by (Yin and Gao, 2014). The model accounts for the deformation in the form of volumetric changes of the annuli resulting from the deformation of the inner and outer casing walls. The following assumptions were introduced by the authors in order to achieve a simplified model:

- "A" annulus pressure is constant.
- "B" and "C" annulus temperatures are roughly equal.
- The annular temperature change is uniform.
- No influx or leakage in each annulus.

The assumption that B and C-annulus are almost equal suggests that any difference observed between the two annuli is neglected. (Yin and Gao, 2014) noticed that by adopting the calculation model of multiple annuli pressure buildup based on micro-temperature increment, it will be more precise to predict the annular pressure buildup. In addition, they concluded that annular pressures varying with temperatures are different at different initial temperatures. More specifically, the rate of pressure increase in high temperature range is faster than that associated with low temperature range. (Jin et al., 2013) have used similar well parameters and through experimental data they presented errors of the order of 10% in APB between measured values and predicted values of casing annulus temperatures and pressures, demonstrating that the model was quite accurate.

3.5.1 Field Data and Models

The incompressible nature of trapped annular fluids implies that minor alterations to temperature, annular volume etc. can lead to significant changes in pressure in completely confined annuli. With such extreme pressures, thick walled casing need to be selected in order to withstand the anticipated collapse and burst loads which should be taken into consideration in regard to casing design for deep HPHT wells (Oudeman and Bacarreza, 1995).

In their paper, (Oudeman and Bacarreza, 1995) showed results of field tests made by Shell Expro (UK) where a battery-operated gauge ran in the annulus between the 9 5/8 in. and the 13 5/8 in. casings of an offshore HPHT well. The aim of the tests was to record pressure and temperature variations throughout drilling, cementing and production operations where pressure can bleed off to surrounding formations. They presented the field test results and compared them to a general model for studying pressure buildup in unconfined sealed annuli in order to correlate the field data. However, the field test results did not show a good correlation with previous models where high annular pressure was predicted. (Oudeman and Bacarreza, 1995) general model formulation for annular pressure buildup was based on three main effects: thermal expansion, change of the annular volume and annular fluid leakoff. With comparison to their calculations made on unconfined sealed annulus, they indicated that leakoff had a dominant influence on the pressure behavior resulting in a quite low local pressure.

However, several years later (Oudeman and Kerem, 2006) studied the transient behavior of Annular Pressure Buildup in sealed annuli of HPHT Wells. A dedicated field test was used to study the annular pressure effect in an appraisal well. They considered the same formulation of (Oudeman and Bacarreza, 1995) that was mentioned previously. They concluded that a considerable increase of annular pressures can arise as a result of the thermal expansion of annular fluids in sealed annuli. Such pressure may rise to a level approaching burst and collapse limits of the casings. Moreover, they concluded that estimates of pressure buildup - mostly pronounced at higher temperatures – when taking into account the effect of ballooning of the outer casing and compression of the inner casing tend to overpredict the pressure buildup rate at higher temperatures. A substantial difference between the actual completion fluid and the pure-base fluid properties or the leak-off of fluids passing through the microannuli between cement sheaths and casings could be the reason behind such overprediction.

3.6 Summary of the Chapter

As can be observed from this bibliographic review, the modeling of thermal phenomena in oil wells brings together the need for specific knowledge in multiphase flows, heat transfer, structural analysis and thermophysical properties.

4 Transient drift flux model

Drift flux model is the flow model used to perform the simulation for this thesis, which can be used to describe one or two phase flow in pipes in one-dimension. The model is transient, which means that it is designed to be able to describe the well conditions changes in time. The drift-flux model can be regarded as an example of nonlinear hyperbolic systems of partial differential equations. The model is governed by two mass conservation laws for each phase, the conservation of the total momentum for the system and four closure laws. Based on the drift flux model, the AUSMV scheme was proposed by (Evje and Fjelde, 2002). This scheme will be presented later in the chapter in more details.

Normally, this model has been used for describing gas-liquid flow but in our case, it will be used to simulate liquid and barite. This will be done by replacing the gas mass conservation law with a barite mass conservation law. A mixture momentum equation will be used for water and barite and the supplying slip relation will be modified to mimic slip between water and barite instead of liquid gas flow.

All the information presented in this chapter are based on the work of (Evje and Fjelde, 2002; Udegbunam et al., 2017) and for further details the reader is advised to consult those papers.

4.1 Conservation laws

The basic idea behind conservation laws is that the amount of a particular physical property of an isolated system is conserved over time. The drift-flux model is used in this thesis to simulate trapped liquid and barite particles mass transport in the closed A-annulus. The model consists of two conservation laws and a mixture momentum equation resulted by adding the momentum equations of the liquid and barite. The following assumptions are made in order to simplify the simulation process:

- The two phases considered in the annulus are water and barite.
- The transient flow is one-dimensional.
- The annular area is assumed uniform and hence the volume change that occur due to annular pressure buildup is uniform as well.

The mass of liquid and barite in the closed annuli will be the same over time and the conservation of mass throughout the system lifetime can be described using the following assumption:

$$Mass_{in} = Mass_{out}$$

However, the following nonlinear partial differential Equations can be formulated expressing conservation of mass and momentum across the annular space.

Conservation of mass for liquid:

$$\frac{\partial}{\partial t}(\alpha_l \rho_l) + \frac{\partial}{\partial z}(\alpha_l \rho_l v_l) = 0 \tag{6}$$

Conservation of mass for barite:

$$\frac{\partial}{\partial t}(\alpha_b \rho_b) + \frac{\partial}{\partial z}(\alpha_b \rho_b v_b) = 0 \tag{7}$$

Conversation of the mixture momentum:

$$\frac{\partial}{\partial t}(\alpha_l \rho_l v_l + \alpha_b \rho_b v_b) + \frac{\partial}{\partial z}(\alpha_l \rho_l v_l^2 + \alpha_b \rho_b v_b^2 + p) = -q \tag{8}$$

Where

$$q = \left(\frac{\partial p}{\partial z}\right)_{fric} + (\alpha_l \rho_l + \alpha_b \rho_b) g \cos\theta \quad (9)$$

Here t is time, and z represents the spatial variable along the A-annulus where the subscripts l and b denote liquid and barite respectively. The variables, ρ_i, α_i, and v_i are the density, volume fraction and velocity of each phase, $i = l, b$. The parameter g is the acceleration due to gravity while θ refers to the wellbore inclination.

The first term on the right side of Equation. 9 is pressure loss due to friction, and the second term is pressure loss due to gravity. It is assumed that the two phases fill the annulus. In this case, $\alpha_l + \alpha_b = 1$. To close the system additional equations (sub models) have to be defined.

4.2 Closure laws

A set of sub models - known as closure laws - are required in order to close the system and solve all the unknown variables in the model. Intuitively, the number of the closure laws must be equal to those that need to be defined in the equations. In the drift flux model, four different closure laws are used:

- Liquid density
- Barite density
- Gas slippage
- Friction model (source term)

Liquid density model

Liquid density is affected by both pressure and temperature. A linearized equation can be utilized to show such relationship and expresses more accurate results for density calculation. For this purpose, liquid density is calculated using the following Equation (Stamnes, 2011):

$$\rho_l = \rho_0 + \frac{\rho_0}{\beta}(p - p_0) - \rho_0 \alpha (T - T_0) \tag{10}$$

Where ρ_0, p_0, and T_0 are the reference point density, pressure and temperature respectively, β is the bulk modulus of the liquid (which is the reciprocal of the compressibility of the liquid), and α is the volumetric thermal expansion coefficient.

For most drilling fluids, the previous Equation is believed to be accurate for pressures in the range of 0 – 500 bar and temperatures, 0 – 200 °C (Stamnes, 2011).

Table 1 bellow gives the density model input parameters for water at the reference point.

Table 1: Bulk modulus and volumetric thermal expansion coefficient for water

ρ_0 (kg/m^3)	p_0 (Pa)	T_0 (°C)	β (Pa)	α (K^{-1})
1000	100000	20	2.2×10^9	0.000207

Barite density

The usual application of the drift flux model is related to gas – liquid flow, hence, we start out with describing this. The gas density is normally calculated using an expression derived from a simplified ideal gas law. Such Equation is expressed by the following expression:

$$\rho_g(p) = \frac{p}{a_g^2} \tag{11}$$

Where a_g is the sound velocity in the gas phase, with an approximated value 316 (m/s), and p represents the pressure in the system.

However, in our case barite is the second phase instead of gas and a simple assumption is used to replace the previous expression. Barite is regarded incompressible and it is assumed that the barite density is 4200 kg/m^3.

Mixture properties

Mixture properties are used in the drift flux model and they include mixtures of density, viscosity and velocity. When initializing the simulation, a certain volume fraction of barite will be assumed (e.g. 0.2) in the annulus, while the total mud density and other mixture properties can then be calculated by:

$$\rho_{mix} = \alpha_l \rho_l + \alpha_b \rho_b$$

$$\nu_{mix} = \alpha_l \nu_l + \alpha_b \nu_b$$

$$\mu_{mix} = \alpha_l \mu_l + \alpha_b \mu_b$$

The distribution of volume between liquid and barite is related by phase volume fraction where the summation of the two fractions is always one and this is shown in the following expression:

$$\alpha_l + \alpha_b = 1$$

Slippage model

As the drift flux model has only one momentum equation, there is a need for another expression in order to provide coupling between water and barite velocity fields. In two phase flow, slip models describe the relative velocity of one phase to the velocity of the other. The gas slip relation can be expressed as follows:

$$v_g = Kv_{mix} + S \tag{12}$$

Here v_g represents the gas velocity where K and S are the distribution coefficient and the drift velocity of gas relative to liquid respectively. The average velocity of the mixture is denoted by v_{mix}. Moreover, K and S values depend on the prevailing flow pattern. When converting this to a model for barite slip vs water, new expressions for K and S will have to be provided. For details on how this can be done, one can consult (Udegbunam et al., 2017).

However, as we only look at the effect of temperature and geometry change due to APB, no settling of barite is considered to take place in the model. In order to ensure no settling of barite we have assumed that K= 1 and S = 0 which imply no slip conditions between the two phases.

Frictional forces

The source term q in Equation (8) can be rewritten in the form:

$$q = F_g + F_w \tag{13}$$

Where F_g represents the pressure loss due to gravity while F_w denotes viscus forces and forces between the wall and fluids.

It is possible to calculate F_w through the following Equation:

$$F_w = \frac{2 f v_{mix} \rho_{mix} \mathrm{abs}(v_{mix})}{(d_{out} - d_{in})} \tag{14}$$

Here d_{out} and d_{in} express the outer and inner diameter of the annular flow area respectivley. In order to get the value of the friction factor f, Reynolds number has to be determined first. Reynolds number, N_{Re}, is used to distinguish between laminar and turbulent flow as the friction factor has different solutions depnding on the flow regime. Reynolds number defines the relation between inertia forces and viscous forces and can be defined as follow:

$$Re = \frac{\rho_{mix} \mathrm{abs}(v_{mix})(d_{out} - d_{in})}{\mu_{mix}} \tag{15}$$

Where Reynolds number is above 3000 ($N_{Re} > 3000$); the flow is turbelent, while if it is below 2000 ($N_{Re} < 2000$); the flow is said to be laminar.

For laminar flow the friction factor is determined by:

$$f = \frac{24}{N_{\mathrm{Re}}} \tag{16}$$

While for turbulent flow it can be estimated using the following formula:

$$f = 0.052(N_{\mathrm{Re}})^{-0.19} \tag{17}$$

The value for the friction factor must be continuous as a function of the Reynolds number. However, if Reynolds number is in the range of (2000 < N_{Re} < 3000), it is quite important to ensure a smooth transition for the friction factor in such transition zone by using interpolation.

However, it can be mentioned that friction will not play a very important role in our case since the fluids will primarily be stagnant in the clsoed A-annulus.

4.3 Numercial Scheme

The Advection Upstream Splitting Method (AUSMV) is a numerical scheme that can present one-dimensional, two-phase transient models. The scheme is based on hybrid flux vector splitting method (FVS). A main aspect of the scheme is its high potential of use for training and academic purposes. It has the required capability to simulate and model a wide range of highly dynamic phenomena related to drilling and production issues such as dual-gradient drilling and underbalanced operations. In addition, it has been used in this thesis to simulate geometrical changes related to annular pressure build-up. However, for further details one can refer to the work of (Evje and Fjelde, 2002).

4.3.1 Discretization process

According to Techopedia[1] , discretization is defined as ''*the process of replacing a continuum with a finite set of points*''. In our context, discretization is a significant process used in order to apply the conservation laws and closure equations that described previously. The well has to be divided first into a certain number of segments where the equations in each segment will be solved separately. Moreover, discretization takes place both in time and space.

Discretization in space

In order to increase the accuracy of the simulation, one has to increase the number of segments. In contrast, more refinment of the model by utilizing large segment number is time consuming and that would be at the expense of computer processeing capacity. However, discretization in the range of 25 to 50 segments is adequate and gives acceptable results for the purpose of this study. It can be mentioned that a second order version of the AUSMV scheme has been used by the application of slopelimiters (Udegbunam et al., 2017), which will be described later. In this way, one can make sure that local variations in pressure and temperature for instance are reflected in the density calculations, which in turn gives the total hydrostatic pressure along the well. The **Figure 4.1** below shows the process of discretization in space where the well (annulus) is divided into a number of segments.

[1] https://www.techopedia.com/definition/1980/discretization

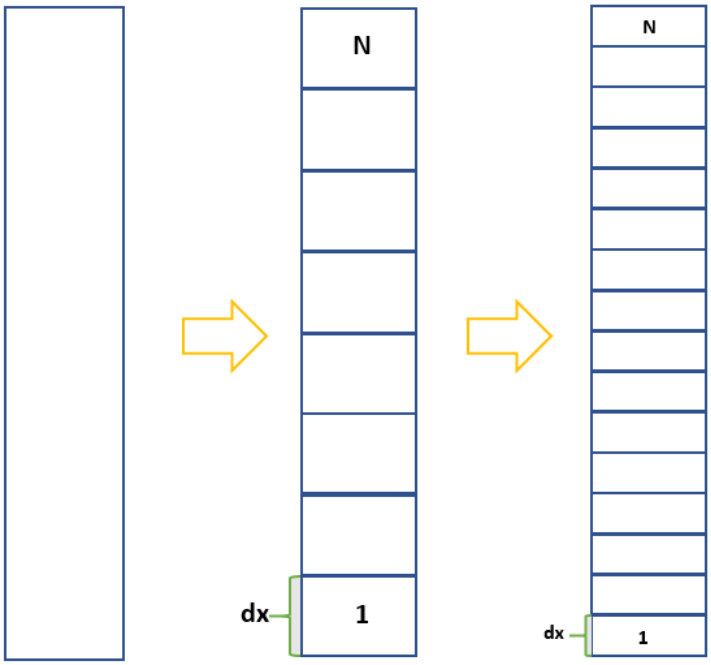

Figure 4.1 Discretization of oil well (or annulus) in space, the arrows refer to more refinement.

Discretization in time

A transient model starts at an initial state where well parameters and flow variables are defined at t_0. Then, the simulation will propagate forward in time, following a specified timestep. Once the calculations for all cells are done, the time is updated by adding one timestep by which the same calculations are made for the next time level. The timestep length - for explicit schemes - is limited by the Courant-Friedrichs-Lewy (CFL) condition that will be explained further in a subsequent point of the chapter.

In order to solve for the conservation laws for different cells at new time level, the conservative variables are updated through the AUSMV scheme using the following expression:

$$U_j^{n+1} = U_j^n - \frac{\Delta t}{\Delta z}(F_{j+1/2}^n - F_{j-1/2}^n) \tag{18}$$

Where

$$U = \begin{bmatrix} u_1 \\ u_2 \\ u_3 \end{bmatrix} = \begin{bmatrix} \alpha_l \rho_l \\ \alpha_b \rho_b \\ \alpha_l \rho_l v_l + \alpha_b \rho_b v_b \end{bmatrix}$$

The indices n and j reflect the timestep and cell number respectively. U is a vector representing the mass and momentum conservative variables defined by the Equations (6) through (8), where they represent the mid values of the cell and are regarded constant within the numerical cells. The flux variable is denoted by F and it describes how mass and momentum are transferred between the cells. However, the fluxes are calculated based on values from the preceding time level, making the scheme explicit. **Figure 4.2** illustrates the process of updating the conservative variables in time. Nevertheless, the formulas for numerical fluxes F will vary between different numerical schemes. Here we have used the formulas defined for the AUSMV scheme which explained in the next section.

However, after the conservative variables have been updated in a cell at a new time level, one has to convert these to physical variables like pressures, densities, phase volume fractions and phase velocities.

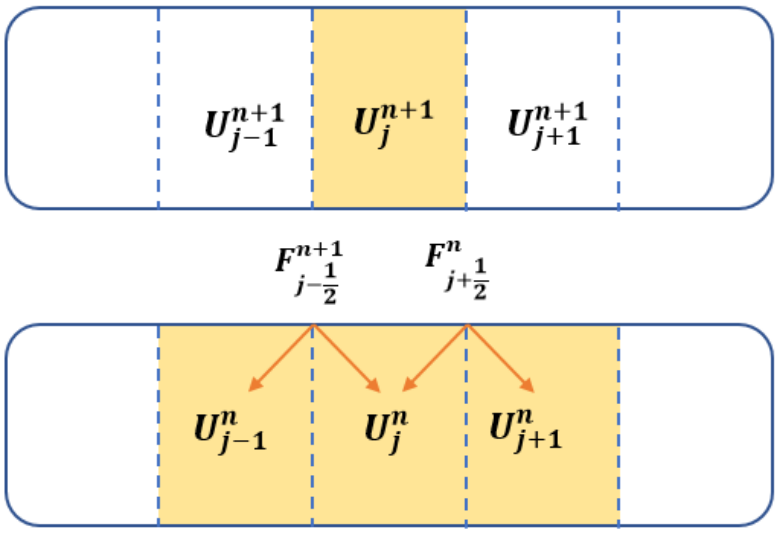

Figure 4.2 Update of discretized variables in time. Edited from (Udegbunam et al., 2017).

4.3.2 Numerical Fluxes & Boundary Treatment

There are several types of explicit schemes in such they vary in the way the fluxes are calculated. Here we have used the AUSMV scheme whereas formulas that regulate the computation process of the fluxes are detailed in (Evje and Fjelde, 2002; Udegbunam et al., 2015).

Depending on well condition, the inlet and outlet fluxes in the boundary cells have to be treated distinctly. Since we are simulating in a closed annulus, no flow will be allowed to leave or enter at the inlet and outlet boundaries where the inlet and outlet mass and momentum fluxes are set to zero. Extrapolation is used to extract the unknown variables from the mid values at the boundary cells. However, in order to determine the annular pressure at the inlet and outlet, the following Equations are used (Udegbunam et al., 2017):

$$p_{inlet} = p(1) + \frac{\Delta z}{2}\rho_{mix} g\cos\theta + \frac{\Delta z}{2}\frac{\Delta p_{fric}}{\Delta z} \quad (19)$$

$$p_{outlet} = p(N) - \frac{\Delta z}{2}\rho_{mix} g\cos\theta - \frac{\Delta z}{2}\frac{\Delta p_{fric}}{\Delta z} \quad (20)$$

4.3.3 Slope Limiters

In the basic AUSMV scheme, numerical diffusion may take place because the scheme has first order accuracy. Numerical diffusion is a phenomenon or a difficulty related to the discretization process in Eulerian simulations where a fixed grid is used. The Eulerian methods in relation to the motion of fluids, focus on specific positions in the space through which the fluid flows as time passes. In such type of simulations, a physical property is characterized as a function of position *x* and time *t*. In the drift flux model time and space are divided into segments whereby mass and momentum equations are discretized into finite difference equations. Numerical diffusion can lead to a situation where the simulated properties behave in a different way than the physical system and will smear out sharp transition zones. For example, the physical sharp interface between a one-phase region and a two-phase region will tend to be smeared out by numerical diffusion. One way to reduce such effect is to increase the number of segments, unfortunately, this would imply more computational time. The more efficient way is to upgrade the scheme from one order to two orders by using slope limiters.

The main idea of slope limiters is that instead of considering the cell boundary variables constant, a slope is used in calculating such values between adjacent cells as illustrated in **Figure 4.3**. These boundary values will in turn be used in defining the fluxes terms. More details can be found in (Udegbunam et al., 2017).

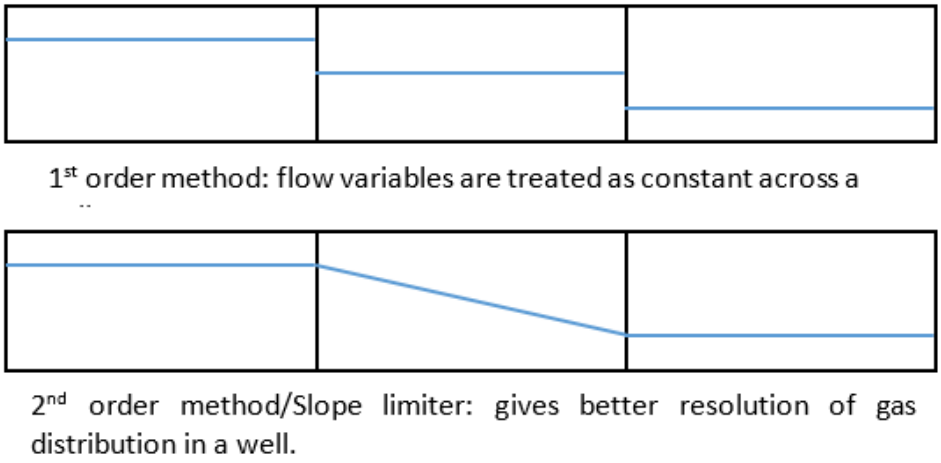

Figure 4.3 Slope limiters concept (Udegbunam et al., 2017).

4.3.4 CFL condition

Since the scheme is explicit, the timestep used in simulation is being limited by the Courant-Friedrichs-Lewy (CFL) condition. CFL condition plays a significant role in relation to solving hyperbolic partial differential equations numerically. It is used to ensure the stability of finite difference equations that model convection or wave phenomena. The time-step length can be limited by following this Relation:

$$\Delta t \leq CFL \frac{\Delta z}{a_{mix}} \tag{21}$$

Where *CFL* is a value between 0 and 1 and depends on the formulation of the numerical scheme, α_{mix} is the speed of the fastest sonic wave in the fluid mixture.

4.3.5 Temperature model

Heat transfer was discussed previously in Chapter 3, where several models to calculate fluid temperature in oil wells have been highlighted. However, a code named ''TACITE'' - based on the drift flux model formulation– was developed to simulate the transient and steady state oil and gas flow in pipelines and production networks (Pauchon and Dhulesia, 1994). An explicit numerical scheme was used for solving the model. The model includes the energy conservation law in addition to mass and momentum equations. TACITE has shown its ability to model the dynamic features of the transient flow with good accuracy. However, one should bear in mind that this model was not developed with respect to having a surrounding formation that can receive and produce heat.

When considering fluid flow in wells one need to model the energy transfer between the rock and the well in a different manner. A way of calculating the temperature in the surrounding rock and the well is to consider a separate model for this. This model will then be solved in conjunction with the drift flux model used for pressure calculations in the well and information will be exchanged between the models. The temperature will become a variable input parameter for the drift flux model based on the simulated results from the dynamic temperature model.

(Petersen et al., 2008) developed a 2-D temperature dynamic model where the thermal computations are offset from other flow related calculations, thus they are not computed simultaneously. However, the model simplifies the dynamic temperature model to be linear by solving the equations simultaneously using a linear equation solver. A similar approach is being applied by John Emeka Udergbunam at the University of Stavanger where a drift flux model and a dynamic temperature model are integrated. The proposed model will be presented in the ASME 37th International Conference on Ocean, Offshore & Arctic Engineering (OMAE), 2018.

A model for APB can be built by combining a drift flux model for the hydraulics taking place in the annuli with a dynamic temperature model. A first attempt in that direction was

presented in (Udegbunam et al., 2017) but the models were not properly integrated at that stage.

In order to have a more realistic model for APB we need to consider geometrical changes in annuli due to annular pressure buildup that is caused by thermal expansion. This thesis can be regarded as an inceptive step to evaluate the capability of the AUSMV scheme to handle such issues. One should note that it is complex to integrate the drift flux model and the dynamic temperature model. The hydraulic model in the annulus will depend on information about the temperature change from the dynamic temperature model. However, the dynamic temperature model again depends on flow variables in the annulus. For instance, the thermophysical properties of the mixture fluid in the annuli will depend on pressure and temperature conditions as well as the concentration of barite. Barite settling have to be taken in consideration in such analysis. These variables will have impact on the heat transfer process between well strings and different annuli and represent information that must be transferred from the drift flux model to the dynamic temperature model. Finally, a model that takes into account variations in geometry due to pressure build up complicates the picture even more.

Nevertheless, for simplicity; no settling is allowed, and a linear temperature buildup is assumed in the simulations presented here since the main objective is to study whether the numerical scheme can handle a geometry that changes with respect to time. In reality, thermal variation is believed to be a slow process where the temperature of the annular fluids changes over a long period of time. However, in order to speed the simulation process and avoid computational difficulties, it is assumed that the temperature buildup goes very fast. The same approach was used by (Udegbunam et al., 2017).

4.3.6 Modeling of geometry changes

Modeling the geometry changes in the A-annulus is the primary objective of this thesis. To simulate such change in the annulus area over time we have assumed that the area change is time dependent. This means that the area or volume of the annulus expands with a certain rate versus time. However, in order to model the geometry change more precisely, such changes should be modeled against the annular pressure. This is more complex and can be done in future work by making some adjustments to the AUSMV scheme to be able to simulate such kind of complexities. The necessary changes and an interpolation formula have been applied to the code and are explained further in the following chapter.

5 Simulations Results

5.1 An Overview

This chapter expresses the parameters used in modeling the geometry expansion due to annular pressure buildup and the Matlab simulation results of the different cases used for the purpose of this thesis.

The AUSMV scheme has been applied to study the effect of geometric expansion of the A-annulus due to increased annular pressure. One of the main objectives is to demonstrate that the scheme can handle transient changes in the geometry and produce reasonable results. To do so, the simulations have been done through several cases and from different perspectives. These cases can be highlighted as follow:

- AUSMV simulation without volume expansion
- Water based annular fluid volume expansion
- Oil based annular fluid volume expansion
- AUSMV simulations with different volume expansion rates
- AUSMV simulations with different barite concentrations

The main goal of these simulations is to simulate geometrical changes in the A-annulus due to APB using the AUSMV scheme based on the drift flux model and compare the results to some previous efforts and studies in the field.

The implemented AUSMV scheme in Matlab and the code used can be found in the Appendix while the changes done to the previous code have been marked with red. The numerical code

for the AUSMV scheme had to be adjusted to simulate the effect of a changing geometry as the pressure increases. A simple model for the volume expansion was implemented to test the capability of the scheme to handle this. This is detailed more later in section 5.4.2.

5.2 Temperature Simulation

As discussed earlier in the previous chapter, the temperature increase is assumed to increase linearly in the A-annulus when production is started, bringing warm fluids from the reservoir to surface. Since the initial temperature in the A-annulus is assumed to follow the geothermal gradient, the temperature increase will be largest at top of annulus while at bottom close to reservoir it will not increase. An illustration of how the temperature on top of annulus increase increases is shown by the simulation results presented in **Figure 5.1** below which is taken from (Udegbunam et al., 2017). In their simulations, a fully dynamic temperature model was considered. The temperature increases almost linearly with time in the beginning of production and then decreases gradually until reaching a steady state condition.

However, in the AUMSV scheme, a fully transient temperature model has not been integrated. Hence, for simplicity, we have assumed that the temperature at different positions in the well increases linearly in time. For the temperature increase at the top of the annulus, the start and end values of the temperature in **Figure 5.1** can be used to define the temperature increase gradient at that position.

Figure 5.2 shows the initial and final temperature profile vs depth which is provided by the simplified temperature model implemented in the AUMSV scheme. This temperature will lead to a pressure build up in the closed A-annulus. It can be mentioned that the initial temperature follows the geothermal gradient starting with bottom seawater temperature at top of the A-annulus since a subsea well is considered.

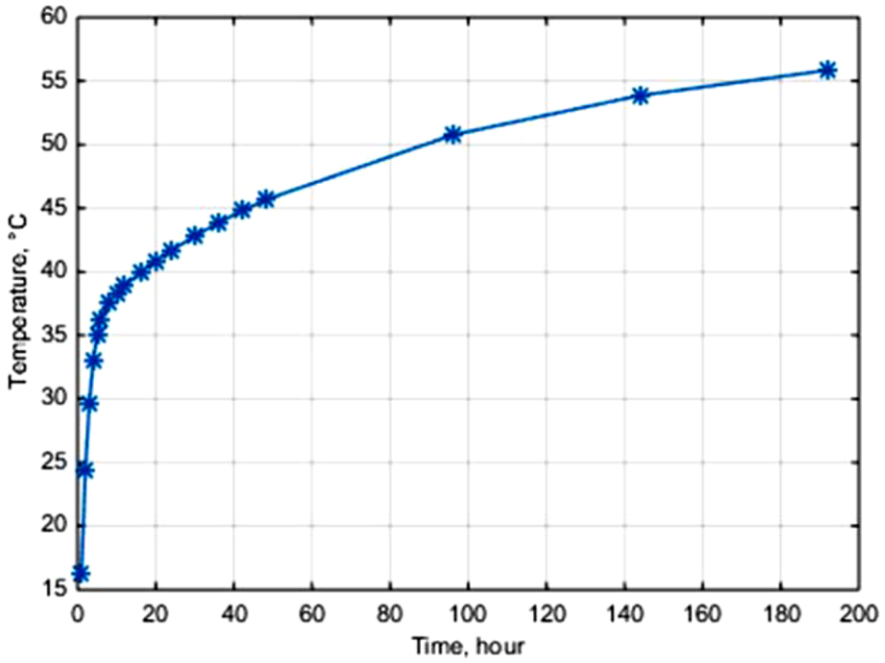

Figure 5.1 Top temperature profile at different production times (Udegbunam et al., 2017).

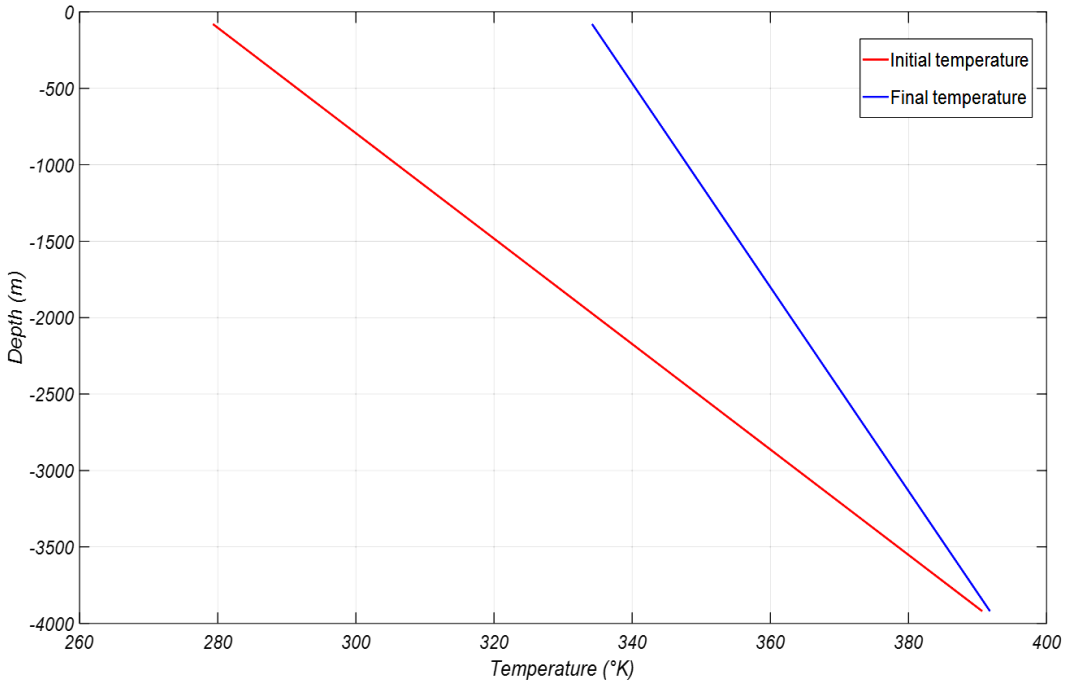

Figure 5.2 Annular fluid initial and final temperature profile vs depth.

5.3 Input parameters

This section presents the different input parameters which used in the simulation process.

Well depth

The well is assumed to be a subsea well with 1000 meters water depth. It is assumed to be vertical and extends 4000 meters below the seabed down to a reservoir. A 9 5/8-inch casing is set just above the reservoir. In addition, a 7-inch production tubing is installed, and a packer locks the tubing to the casing just above the reservoir. On top, a subsea XMT is installed. Hence, a 4000-meter-long A-annulus is formed.

Annular diameters

The A-annulus outer diameter which represents the production casing inner diameter is set to 0.21662 m (ID of 9 5/8 inch production casing) while the annular inner diameter which is the production tubing outer diameter is 0.1778 (OD of 7 inch production tubing). It is assumed that the cross-sectional area is uniform through the whole space which implies a uniform geometry change as well.

Fluid selection and properties

In order to simulate APB for different fluids, both water and oil based annular fluids have been used. In both cases, barite is assumed to be the weighting material (the second phase in the drift flux model). Either water or oil is the base fluid (first phase in the AUSMV scheme). The barite concentration is assumed to be 20 % of the total volume. The barite concentration is assumed fixed neglecting any settling tendencies of barite. Hence, there will be no slip

conditions between the base fluid and the barite. However, the fixed barite concentration is changed in the last section of this chapter to study its influence on the rate of annular pressure buildup. **Table 2** below represents the density and viscosity parameters of the different phases.

Table 2: Fluid properties of water and oil

Fluid type	Density (kg/m3)	Viscosity (Pa*s)
Water	1000	0.001
Oil	870	0.001
Barite	4200	0.001

All densities are assumed at 20 °C. In addition, mixture viscosities are assumed to be equal to the viscosity of water. However, there is no considerable influence of the viscosity as no friction in the annulus is allowed.

The liquid density is calculated using the following Equation of (Stamnes, 2011) as explained in the previous chapter. The model has been implemented for both water and oil based annular fluids.

$$\rho_l = \rho_0 + \frac{\rho_0}{\beta}(p - p_0) - \rho_0 \alpha (T - T_0)$$

Where ρ_0, p_0, and T_0 are the reference point density, pressure and temperature respectively, β is the bulk modulus of the liquid (which is the reciprocal of the compressibility of the liquid), and α is the volumetric thermal expansion coefficient.

Initialization and Fluid mass rate at the Boundaries

The initial conditions in the A-annulus are based on assuming a stagnant liquid. The mass rate vs time of the different fluids is set to zero at the boundaries since no fluid is flowing in or out of the system since we have a closed system.

Well discretization

The well is divided into segments. The number of cells or boxes in the well is set to be 25. However, the number of boxes were also varied from 50 up to 200 but no significant changes were noticed. The timestep is 0.02s in the case of 25 boxes and 0.01s when using 50 boxes and so on. Nevertheless, we must always half the timestep if we double the number of boxes. This is to ensure that the CFL conditions is satisfied to avoid unstable simulations. In all simulations, the CFL number is being fixed to a value of 0.1875.

Regarding the simulating time, the duration of simulation is set to be around 1900s where the simulation begins at t=0 and ends at t=1900. However, the simulations in the first 100 seconds are not considered and let mainly to stabilize the system. It can be mentioned that the temperature buildup assumed in the simulations has been speeded up compared to what will be seen in reality. This was done to save computation time and the results would be the same.

Annulus temperature

A linear model is used for temperature modeling. It is assumed that the annulus temperature increases linearly with time with different magnitude of build up at different depths. The following formula is used to calculate the geothermal gradient:

$$\text{tempgradient} = (\text{tempbot} - \text{temptop})/\text{welldepth} \quad (22)$$

where:

tempgradient = the geothermal gradient,

tempbot = initial temperature at bottom of A-annulus = 120 °C or 393 °K,

temptop =initial temperature at top of A-annulus = 4 °C or 277 °K

However, when production has heated up the annulus, the final temperature at top of the A-annulus is assumed to reach 60 °C. the temperature gradient with depth is calculated by similar formula as the previous one, while the temperature buildup versus time is computed as follow:

$$\text{tempbuilduptimegradient}(i) = (\text{tempfinal}(i) - \text{temptop}(i))/\text{timeperiod} \quad (23)$$

where the index (i) refers to the box number while the timeperiod for buildup temperature is assumed 1000 seconds to speed up the simulation process.

5.4 Simulation Results

5.4.1 AUSMV simulation without volume expansion

Due to hot production fluids flowing from the reservoir up to surface, the temperature of the fluid trapped in the A-annulus increases, and as a result these fluids are subjected to thermal expansion that will cause APB. The following two **Figures** show the annular pressure buildup of the A-annulus over the simulation time 100 – 1900s for the base case. **Figure 5.3** represents the top pressure against time, where no buildup is allowed in the first 100s in order to allow the system to reach a steady state. This is done to stabilize the simulation and to make sure that no errors arise along the process. It is clear that the top pressure has increased linearly and in smooth manner from 100 bar (the pressure at the seabed) to about 330 bar at the end of the simulation.

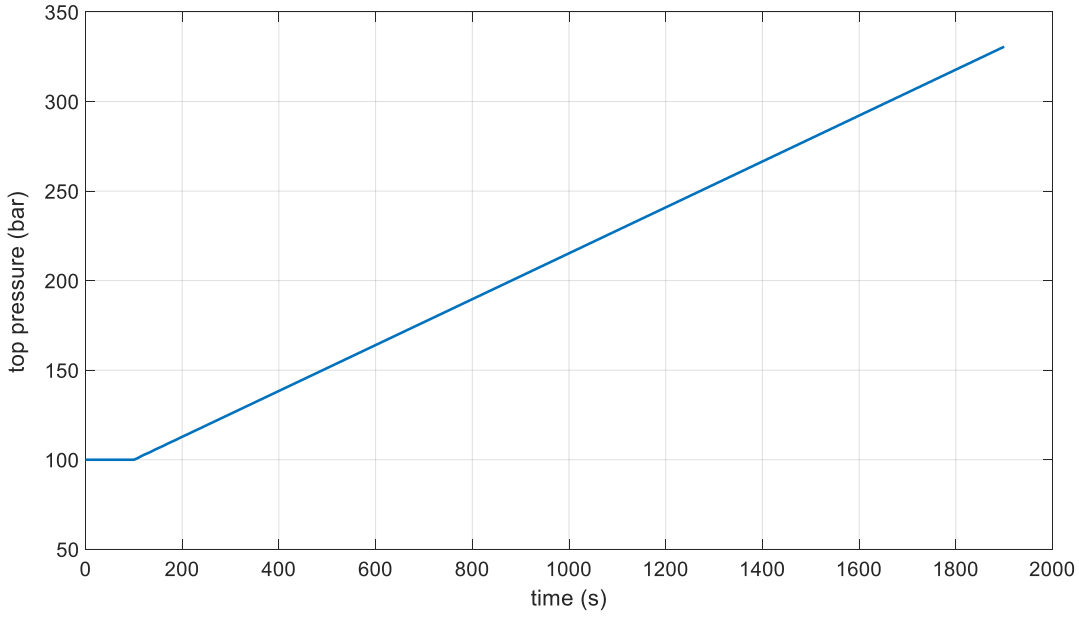

Figure 5.3 Top pressure vs simulation time, water based and no geometry expansion.

The process is repeated to investigate how much the increase in pressure would be at the inlet or the bottom of the annulus. The result is shown in **Figure 5.4** and it can be seen how the bottomhole pressure has increased from around 750 bars at t=100s to approximately 980 bars at the end of the simulation at t=1900s.

It is noticed that the pressure has increased by around 230 bars both at top and bottom of the A-annulus. Such increase might be a challenge for the surrounding casing and tubing and may have a serious impact on the well integrity. It can lead to burst of the outer casing and collapse of the inner tubing. Moreover, there will be a long-term pressure buildup due to the settling of the barite that is neglected in our simulations for the purpose of this thesis. However, the major influence on the overall APB comes from the increase in temperature.

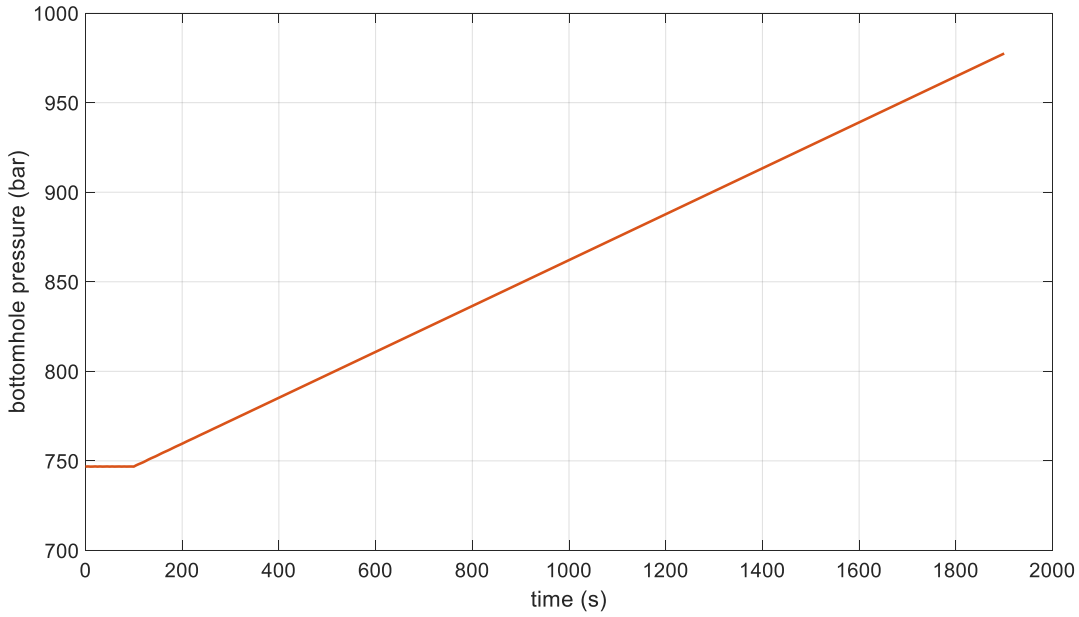

Figure 5.4 Bottomhole pressure vs simulation time, water based and no geometry expansion.

5.4.2 Water based annular fluid volume expansion

The main idea of this thesis is to investigate the ability of the AUSMV scheme and drift flux model to handle the volume expansion or area change that might be applied on closed annuli due to the effect of APB. In order to implement such change in the area with time we have assumed that the area change is time dependent. This means that the area or volume of the annulus expands with a certain rate over time. Interpolation technique has been used in order to achieve a reasonable increase in the annulus area that would comply with results of similar previous studies such as (Alcofra et al., 2014). The necessary changes and interpolation formulas have been applied to the code and can be found in the Appendix. The interpolation formulas used for area calculation are defined in a way that the outer annulus diameter (casing inner diameter) increases while the inner annulus diameter (tubing outer diameter) decreases with the same rate as follow:

$$\mathrm{Do} = \mathrm{do} + \frac{\mathrm{time} - 100)}{\mathrm{endtime} - 100} * 0.0007 \tag{24}$$

$$\mathrm{Di} = \mathrm{di} + \frac{\mathrm{time} - 100)}{\mathrm{endtime} - 100} * 0.0007 \tag{25}$$

Where Do and Di are the calculated outer and inner annulus diameters, while do and di represent the original outer and inner annulus diameters respectively. The endtime is the total simulation time and it equals 1900 seconds. The rightmost value in the interpolation Equations gives the required increase in volume, (for example 0.0007 in this case gives about 3.6% increase in the original volume).

Then the area can be calculated as:

$$Area = \frac{3.14}{4}\ (Do^2 - Di^2) \tag{26}$$

And the annular volume can be obtained by multiplying the new area by the total length of the annulus which is 4000m. The increase percentage in volume then is calculated as follow:

$$dV = \frac{\text{new annular volume} - \text{original annular volume}}{\text{original annular volume}} * 100 \tag{27}$$

(Alcofra et al., 2014) have studied the annular pressure buildup in oil wells where they coupled the volume change of the annuli fluids with the associated volume change in casings. They concluded that the overall volume changes by around 3.59% in the A-annulus while this percentage decreases gradually in the subsequent annuli. In their study, oil was chosen as the main fluid that fill the annuli and the model of (Sorelle et al., 1982) was considered as the density model. Here we have used their findings as a guidance to help us in our simulations of annular volume change.

Similar well configuration has been used as presented before with the same well parameters as well. The drilling fluid used in this case is a mixture of water and barite. No mass flow is allowed in or out of the system, thus the boundary mass rates are set to zero. Different rates of annular volume expansion are used in order to come up with reasonable results at the end of the simulations. However, after many trials we could come up with the maximum volume change that gives relatively realistic results. This volume expansion represents about 0,5% increase of the original annular volume for 1800 seconds of simulation when using water based annular fluid. Using higher rates would result in negative pressure buildup in the AUSMV scheme which can be noticed clearly in **Figures 5.5** and **5.6** for the top and bottomhole annular pressures against time. It can be also noticed how the results show a

decline in the pressure instead of buildup which indicate an error in the simulation parameters reflected by the introduced area change. The occurrence of negative pressures is highly unphysical. The reason can be that we actually allowed to annular volume to expand too much compared to what would be physically possible and should be checked with a physical model for how much geometry will change for a given pressure increase (Halal and Mitchell, 1994). It is difficult to conclude that the problem is related to the scheme itself at this stage.

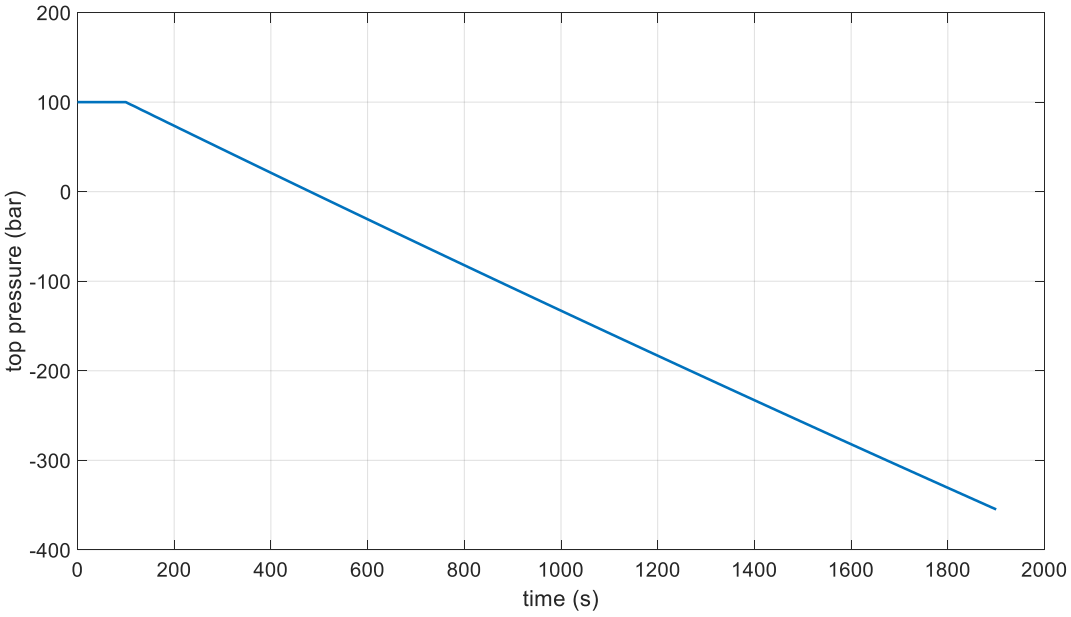

Figure 5.5 Top pressure vs simulation time, water based with 2.57% volume increase.

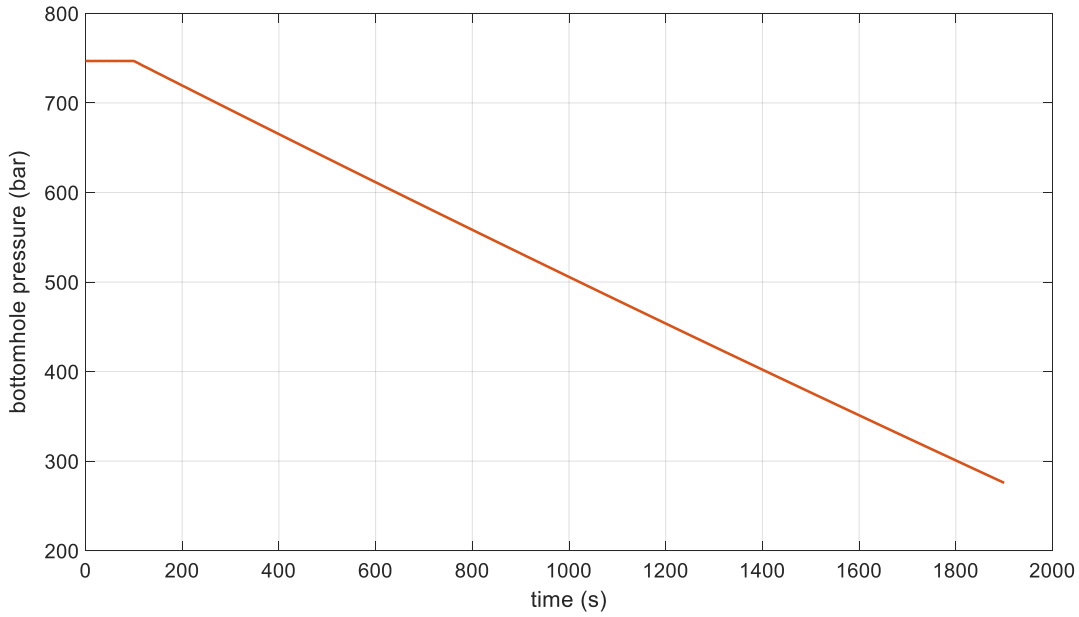

Figure 5.6 Bottomhole pressure vs simulation time, water based with 2.57% volume increase.

Nevertheless, **Figures 5.7** and **5.8** show the simulation results of the first positive buildup where the volume change increased by about 0,5% of the original annular volume. The top pressure has increased by 90 bars from 100 to approximately 190 bar, while the bottomhole pressure has experienced around 86 bar pressure buildup from about 747 to 833 bar at the end of the simulation time. If we compare this to the base case, we observe that the pressure buildup has been reduced from 230 bar to around 90 bars which is a large reduction. Hence it is important to have a good model for this expansion effect of the geometrical volume.

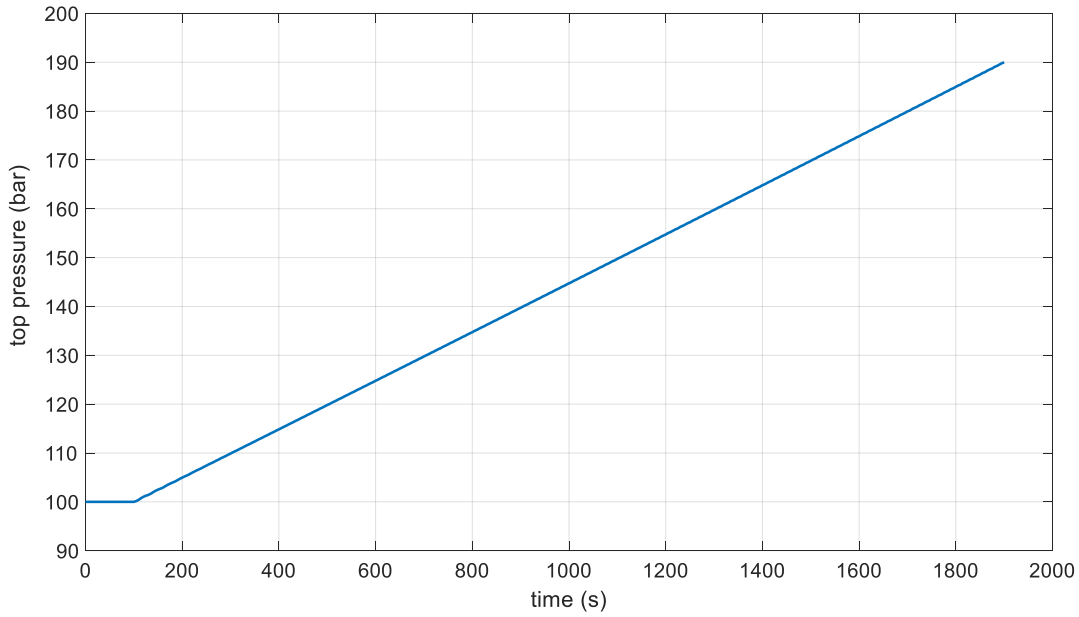

Figure 5.7 Top pressure vs simulation time, water based with 0.5% volume increase.

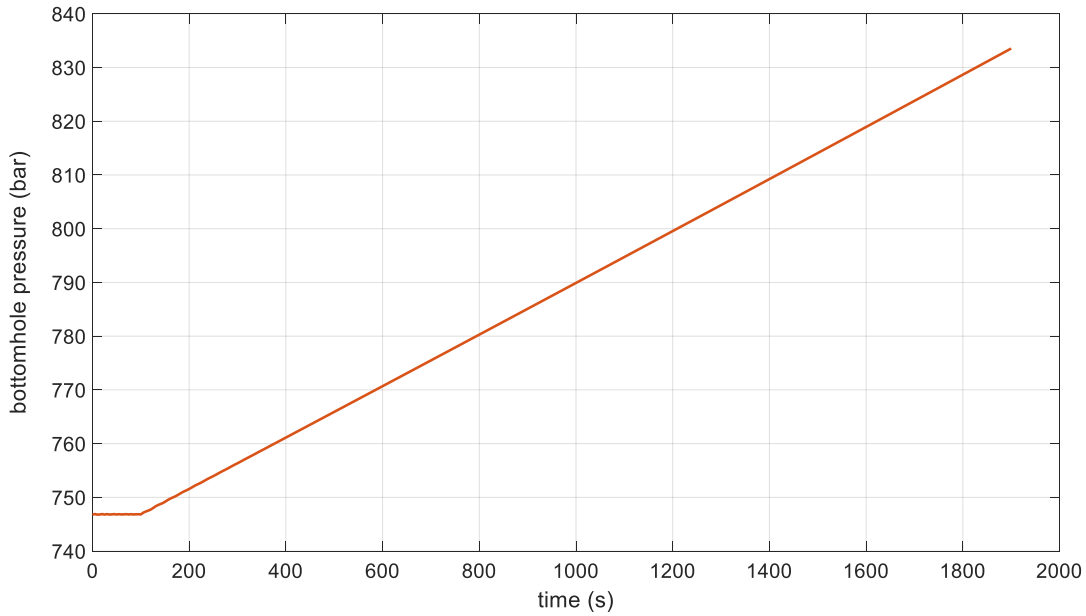

Figure 5.8 Bottomhole pressure vs simulation time, water based with 0.5% volume increase.

5.4.3 Oil based annular fluid volume expansion

It has been noticed that by changing the annular fluid type, a notable change in the pressure buildup takes place. In the case of using oil based annular fluid we were able to make our simple volume change model to have the same volume expansion of 3.59% increase in the A-annulus as was modelled in (Alcofra et al., 2014). However, it is prudent to remark that the rate of annular pressure buildup varies with the variations in the values of β and α in the liquid density model. Where β represents the bulk modulus of the liquid (which is the reciprocal of the compressibility of the liquid), and α is the volumetric thermal expansion coefficient as mentioned previously.

A simple sensitivity analysis was done by selecting five different values for the parameters β and α in order to investigate their influence on the pressure buildup of the trapped annular fluids. A constant volume expansion is applied in all simulations that is around 3.59% increase in the original annular volume which is motivated by (Alcofra et al., 2014). The used parameters and results are presented in **Table 3**, where **Figure 5.9** shows the corresponding outcome. Here all pressure variations are given in relation to the initial conditions of the simulation. It can be noticed how a small change in the values of β or α can increase the rate of the annular pressure buildup significantly. It can be noticed that with keeping the β parameter constant, a minor increase in the α value from 0.00095 to 0.00099 has increased the pressure buildup by around 28 bar from 86.4 to 114.5 bars. Increasing α will lead to larger pressure build up since the fluid will have a tendency to expand more**.** Similarly, the APB has increased as well when varying the β from 1.3*10^9 to 1.66*10^9 while fixing the α value to 0.00095. According to the model of (Moe and Erpelding, 2000), Increasing α reduces the density which means increased theoretical fluid volume expansion and hence a larger pressure build up while increasing β leads to reduce the fluid compressibility and hence increase the pressure build up accordingly.

Table 3: The effect of density model parameters on the APB

α (K^{-1})	β *10^9 (Pa)	Change in volume (%)	Top pressure variation (bar)	BHP variation (bar)	Average APB
0.000764	1.66	3.59	-38.7	-57.5	-48.1
0.00095	1.66	3.59	188	172	180
0.00095	1.3	3.59	96	76.8	86.4
0.00099	1.3	3.59	123	106	114.5
0.00125	1.05	3.59	243	219	231

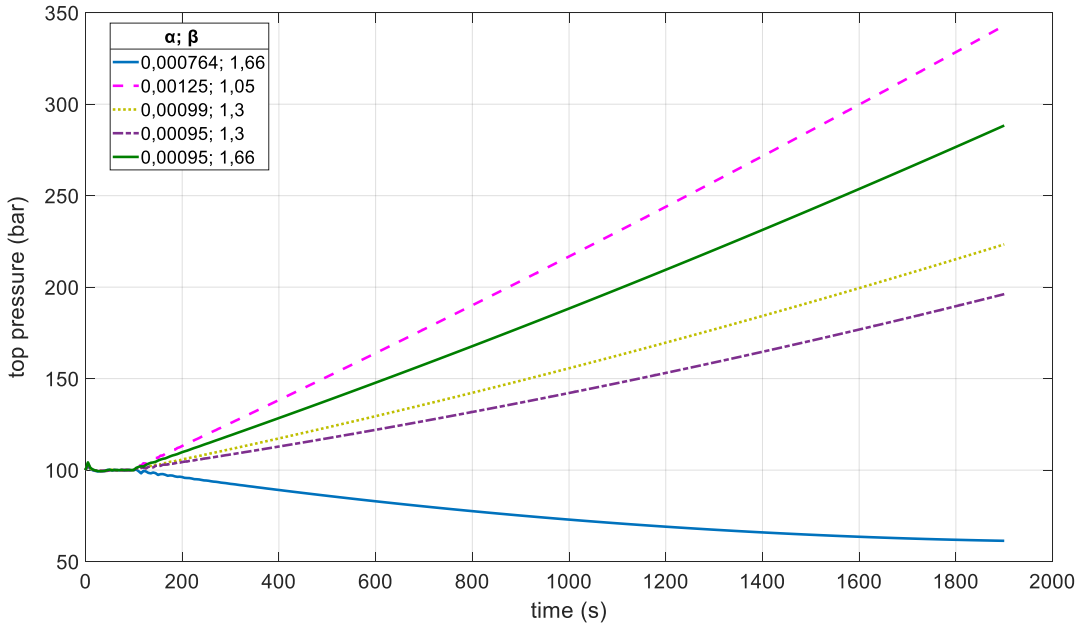

Figure 5.9 Top pressure vs time, oil based with 3.59% volume increase using different β and α values.

Water vs oil based annular fluid

A comparison between the water and oil based annular fluid has been done in relation to annular pressure buildup when all other conditions are the same. **Table 4** shows the liquid density input parameters in this case. We assumed no geometry expansion and the same temperature build up for both systems. Also, the most likely parameter for oil based fluids are selected. From **Figure 5.10**, it can be seen a larger pressure buildup when using oil based fluids in comparison to water based fluids that involve less APB. This can be referred to different thermal and bulk parameters for the two distinctive fluids and hence different thermal expansion of the fluids with a different pressure build up. These two effects are related to the thermal coefficient and the bulk parameter of the fluid.

Table 4: Water and oil density model input parameters

Fluid type	ρ_0 (kg/m^3)	p_0 (Pa)	β (Pa)	α (K^{-1})
water	1000	100000	2.2×10^9	0.000207
oil	870	100000	1.66×10^9	0.000764

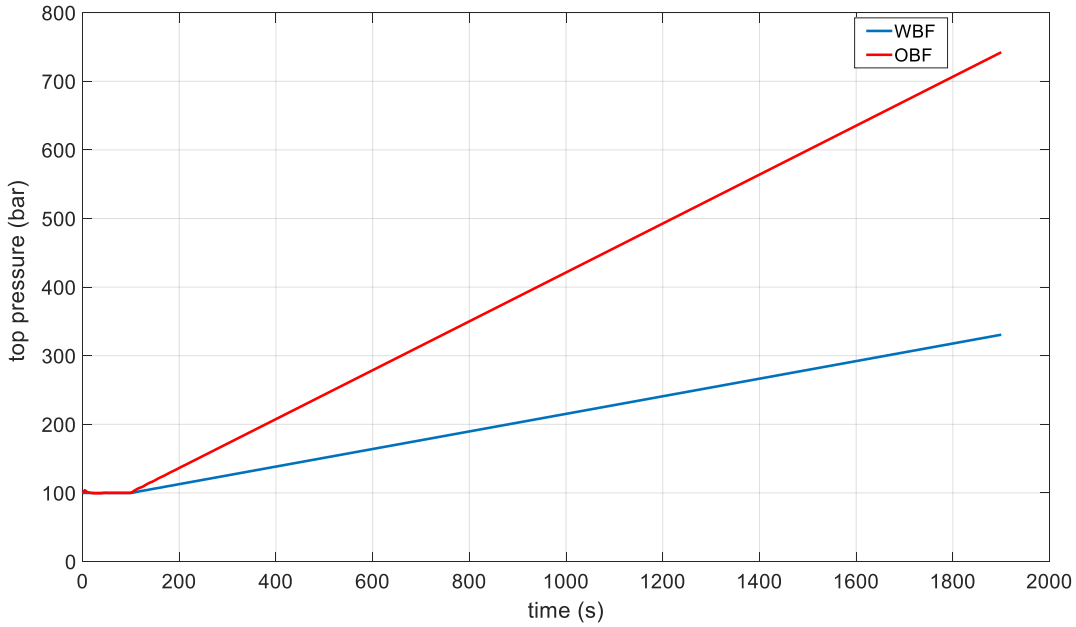

Figure 5.10 Top pressure vs time when using water based annular fluids (WBF) vs oil based annular fluids (OBF), no geometry expansion.

5.4.4 AUSMV simulation with different volume expansion rates

The following simulations are aimed to investigate the influence of using various volume expansion rates on the annular pressure buildup while fixing β and α parameters. In the **Figure 5.11** below, three different annular volume expansion values are compared with respect to how the pressure build up will be on the top of the A-annulus. The trapped annular fluid is assumed oil base where β is set to $1.66*10^9$ and α is 0.000764 for the three simulation cases where the volume expansion rate varies. It can be clearly seen how the AUSMV scheme has shown that the annular volume expansion relates to annular pressure buildup rate with a reverse relationship. This means that as the annular volume increases, a decrease in the rate of the annular pressure buildup will take place consequently. However, it can be noticed that the annular pressure buildup rate decreases when there is a significant volume increase in the annulus which is clear in the **Figure 5.11**when there is about 3,59% annular volume

expansion. This is unphysical since the only thing that can increase the volume is an increase in pressure. Nevertheless, the results will be different to some extent depending on the type of the annular fluid where the density and compressibility parameters vary.

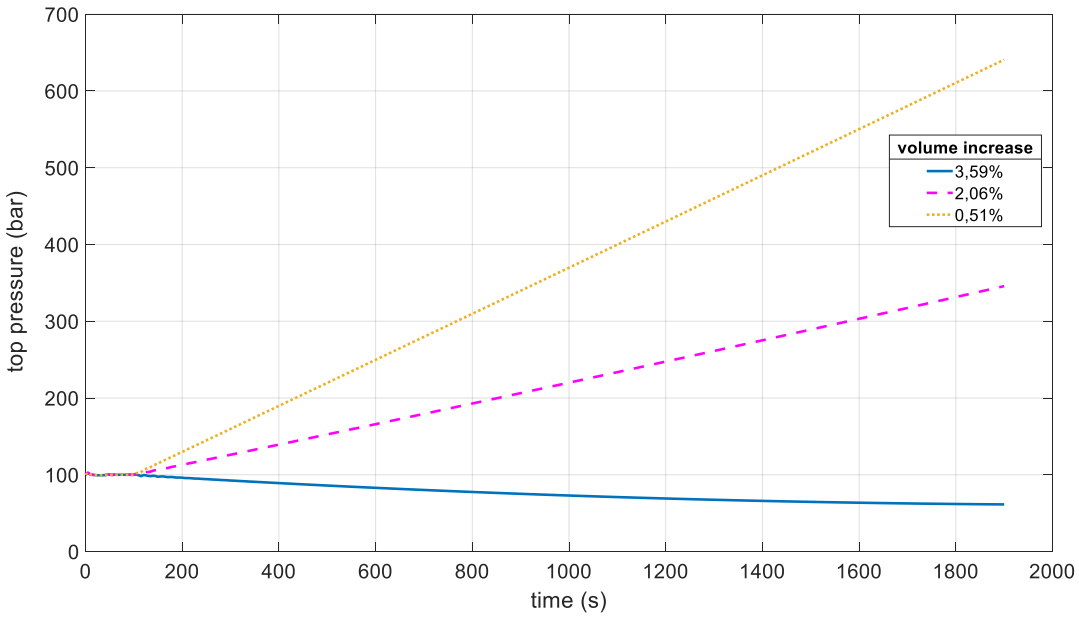

Figure 5.11 Top pressure vs time, oil based with different volume expansion rates.

5.4.5 AUSMV simulation with different barite concentrations

All the previous simulations were based on a fixed volume phase fraction where the liquid phase represents 80% while the barite is 20% of the total annular volume. Still, no barite settling is considered. However, we want to investigate what can happen if we change this percentages and how such changes would affect the rate of annular pressure buildup. Indeed we should expect the pressure build to be different since the mixture fluid compressibility will be different. Only the liquid phase is compressible. This will also impact the mixture density which also has some impact on the compressibility of the fluid with respect to pressure. To do so, three different phase volume scenarios have been considered where the

total increase in volume expansion is set to be around 0.5% of the original annular volume. The liquid volume fraction – which is water in this case – varies as 90%, 80% and 70% of the mixture volume which in turn implies 10%, 20% and 30% barite volume fractions accordingly.

Figures 5.12 and **5.13** show the three scenarios with the top and bottomhole annular pressure. It can be seen from both **Figures** that the rate of annular pressure buildup increases as a result of decreasing barite volume in the mixture. The total pressure buildup in the top of the annulus in this case are around 70, 90 and 105 bars where the barite concentrations were 30%, 20% and 10% respectively. A similar trend can be seen when comparing the total bottomhole annular pressure build up for various barite concentrations. However, it is clear how the initial bottomhole pressure increased as a result of the change in the total density of the annular fluid. Moreover, it is important to take into consideration the incompressibility of barite and how that affects the overall compressibility of the mixture fluid. As the barite is incompressible, increasing this concentration would impact how much fluid volumes that can be expanded. With larger volumes of barite, less volume of liquid will be subject to volume expansion due to temperature and the pressure build up will become less.

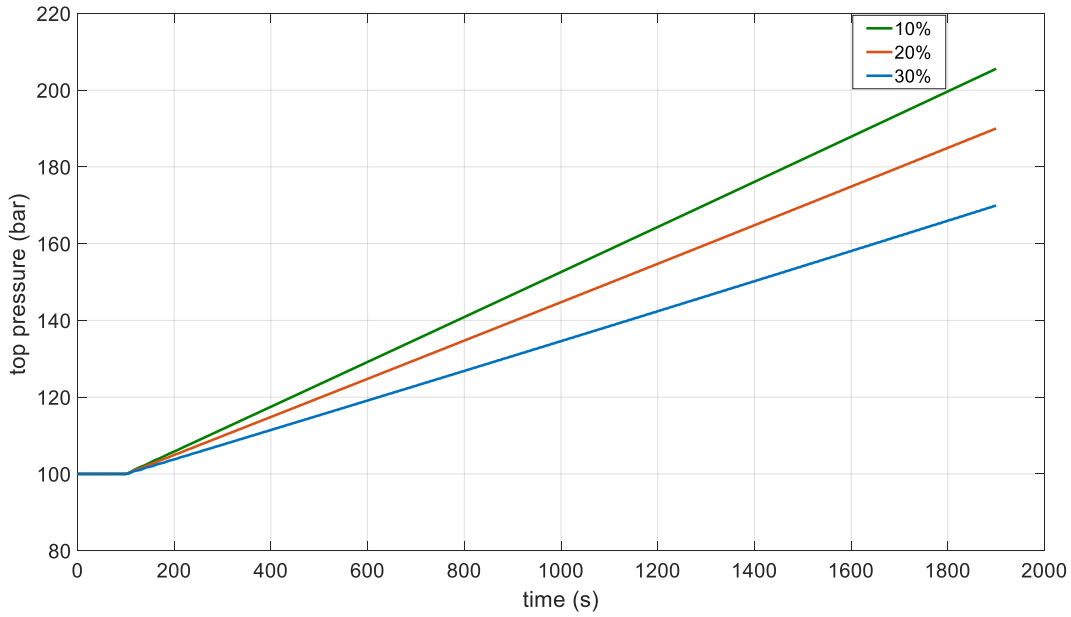

Figure 5.12 Top pressure vs time, oil based with different barite concentrations.

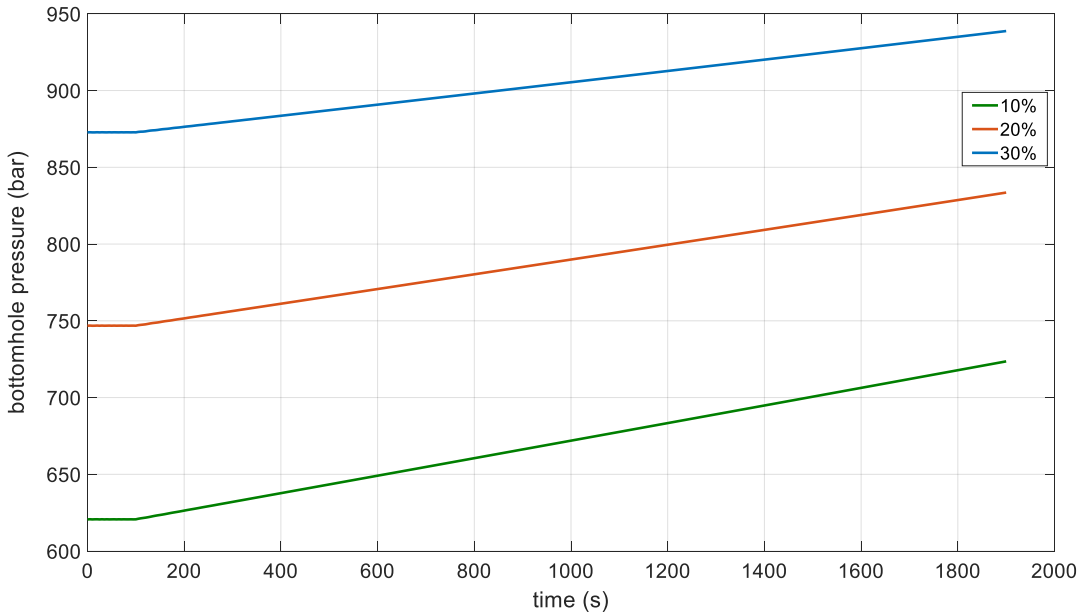

Figure 5.13 Bottomhole pressure vs time, oil based with different barite concentrations.

6 Conclusion and Further work

6.1 Conclusions and main findings

The original AUSMV scheme has been modified in order to simulate geometrical changes in wells and annuli due to annular pressure buildup effect. The AUSMV has shown its ability to model annular volume changes without numerical problems considering a simple model for the geometrical volume expansion. Overall, the scheme can be regarded as a robust and reliable tool for such kind of simulations.

It is known that the annuli trapped fluids experience thermal expansion when subjected to APB which in turn apply stresses on the surrounding casings and tubing that may affect the well integrity harmfully. In order to model the annular volume expansion, we have assumed that the area change is time dependent. We have just expanded the area by a certain rate versus time. However, by this way we could simplify the simulation process and at the same time achieve acceptable results as the area was assumed to increase at the same time as we assumed that the temperature increased.

Several conclusions and findings can be drawn from the simulation results in this thesis as follows:

- The AUSMV scheme is a straightforward tool for modeling two phases, one dimensional flow. It has proved the capability to simulate annular pressure buildup in closed annuli with high reliability with respect to robustness. In addition, the AUSMV scheme has shown its ability to handle the geometrical changes that may take place in closed annuli due to APB. The simulations have shown in general that adding the possibility for geometrical volume expansion as the pressure and temperature builds up will lead to a lower APB compared to the base case where no geometrical changes are allowed.

- The type of fluid filing the annular space plays a significant rule in regard to annular pressure buildup. Oil based fluids have shown higher values of pressure buildup in term of magnitude and rate compared to water based fluids. Essentially, an increase in the annular pressure buildup rate was expected due to different bulk modulus and thermal expansion coefficients. Nonetheless, the AUSMV scheme showed different response of the two liquids to the volume expansion. Water has expressed high sensitivity to the implemented change in geometrical volume whereby a relatively high geometrical volume expansion in the A-annulus gives a reduction in the annular pressure which is physically unrealistic. However, there was a positive buildup in the annular pressure by applying larger geometrical volume expansion using oil based fluids. Our geometrical volume expansion model is very simplistic and when we obtain a reduced pressure in the well; it is clear that the assumed volume increase has been too large. There should be no volume expansion if there is no pressure build up. Hence, a more realistic model for this is needed. The reason why oil and water have different sensitivity with respect to how much geometrical volume that can be induced without producing unphysical results is related to the fact that the fluids expand differently.

- The liquid density model parameters play a significant role in the relation between APB and the annular volume change. In the oil case, five different values for each parameter β and α were selected in order to investigate their influence on the pressure buildup of the trapped annular fluids. A constant geometrical volume expansion was assumed in all simulations which is around 3.59% increase in the original annular volume. The results have shown that slight growth in the values of β or α can increase both the magnitude and rate of the annular pressure buildup significantly.

- The AUSMV scheme was used to investigate the influence of using various volume expansion rates on the annular pressure buildup where β and α are constant. The simulation results have exposed that the annular volume expansion relates to the

annular pressure buildup rate with a reverse relationship. More precisely, as the annular volume increases there will be a decrease in the rate of the annular pressure buildup. However, the results can be different depending on the type of the annular fluid where the bulk modulus and thermal expansion coefficients vary.

- The AUSMV scheme was employed also to investigate what can happen if we change the barite concentration and how such change would affect the rate of annular pressure buildup. The total increase in geometrical volume expansion was set to be around 0.5% of the original annular volume. The results have proved that the rate of annular pressure buildup increases as a result of decreasing the barite volume in the mixture. With larger volumes of barite, less volume of liquid will be subject to volume expansion due to temperature and the pressure build up will become less.

6.2 Recommendations and Further work

The liquid density model used in this thesis is based on the simple model of (Stamnes, 2011) which is basically a linearized equation of state with doubtful accuracy in high pressures or high temperature. In this thesis, a simple fluid consisting of water and barite without additives was assumed. In addition, we have used the same simple model for oil based fluids by just modifying the reference density, β and α parameters. However, oil based drilling fluids may compose of oil, water in addition to gellants, wetting agents and other materials. In future work, the AUSMV might be extended to include more complex density models that can simulate - with more precision – both water and oil based annular fluids used in existing oil fields.

In this way, the first mass conservation law would be occupied with the entire mud fluids while the other could be used for eventual gas leakages in the annuli (gas phase). However, this version of the AUSMV scheme would not be able to simulate settling of barite since the

barite is mixed into the mud and does not experience slippage. Another alternative is to keep the structure without change but let the fluid density model incorporates both water and oil in the first mass conservation law while the second conservation law can be occupied by barite. Nevertheless, if one wants to include slippage, all phases should be placed separately in the two mass conservation laws. And the slippage model - in the closure laws - that replaces the lack of two separate momentum equations can handle the slippage between the phases.

While in this thesis no barite settling is allowed to take place through the simulation process, (Udegbunam et al., 2017) has shown the ability of the AUSMV scheme to simulate APB where also the effect of barite settling is taken into account. In fact, barite settling alters the thermal properties of the mixture fluid in the annulus which again can impact the APB. For more improvement in the simulation results, both geometry change in sealed annuli and barite settling are recommended to be included in the model. This is believed to help achieving better prediction of the APB.

In oil fields, a typical well consists of several casings and production tubing where there is a number of annuli in between filled with fluids of different properties. Moreover, heat transfer will vary through the different annuli and hence the thermal expansion of annular fluids will not be the same. In addition, casings and tubing may vary in their response to thermal expansion due to different yield strengths and the interdependency over the strings behavior. Thus, there will be variation in response to expansion and reduction in volume.

This issue has been discussed in chapter 4 where it was shown how (Halal and Mitchell, 1994; MacEachran and Adams, 1991) among others have emphasized the need for multistring analysis rather than the existing single-string models. Correspondingly, they have introduced some methods to analyze the deformations of multiple casings. However, a single annulus has been under consideration in this thesis for simplicity. As a recommendation for future work, the AUSMV scheme can be extended to include such complexity and combine all the previous factors in the overall geometrical changes in order to obtain more reliable simulations.

References

Aadnøy, B.S., 2011. Modern Well Design. Taylor & Francis Group, LLC, Boca Raton, Florida.

Aadnøy, B.S., Cooper, I., Miska, S.Z., Mitchell, R.F. and Payne, M.L., 2009. Advanced drilling and well technology. SPE.

Adams, A., 1991. How to design for annulus fluid heat-up, SPE Annual Technical Conference and Exhibition. Society of Petroleum Engineers.

Adariani, Y.H., 2012. Experimental Study and Modeling of Barite Sag in Annular Flow. The University of Tulsa.

Alcofra, E.L.M., Nieckele, A.O. and Lage, A.C.V.M., 2014. Annular Pressure Buildup in Oil Wells, In the Proceedings of ENCIT 2014–15th Brazilian Congress of Thermal Sciences and Engineering, Belem, Brazil.

Alves, I., Alhanati, F. and Shoham, O., 1992. A unified model for predicting flowing temperature distribution in wellbores and pipelines. SPE production Engineering, 7(04): 363-367.

API recommended practice 96, 2013. Deepwater Well Design and Construction. (first edition).

Azzola, J., Tselepidakis, D., Pattillo, P.D., Richey, J.F., Tinker, S.J., Miller, R. and Segreto, S.J., 2007. Application of Vacuum Insulated Tubing to Mitigate Annular Pressure Buildup. SPE Drilling & Completion, 22(01): 46-51.

Barcelos, J.G.A., Hafemann, T.E., Ferreira, M.V.D., da Silva, A.K. and Barbosa Jr, J.R., 2017. A new approach for calculating annular pressure buildup in an offshore well. IV Journeys In Multiphase Flows (2017), March 27-31, São Paulo, Sp, Brazil.

Bendiksen, K.H., Maines, D., Moe, R. and Nuland, S., 1991. The dynamic two-fluid model OLGA: Theory and application. SPE production engineering, 6(02): 171-180.

Bradford, D., Gibson, D., Gosch, S., Pattillo, P., Sharp, J. and Taylor, C., 2002. Marlin failure analysis and redesign; part 1, description of failure, IADC/SPE Drilling Conference. Society of Petroleum Engineers.

Ellis, R., Fritchie Jr, D., Gibson, D., Gosch, S. and Pattillo, P., 2002. Marlin failure analysis and redesign; part 2, redesign, IADC/SPE Drilling Conference. Society of Petroleum Engineers.

Ettehadi, O.R., Miska, S.Z., Ozbayoglu, M.E., Takach, N.E., Coe, D. and Chen, D.C., 2014. Annular pressure build up (APB) analysis-optimization of fluid rheology, SPE Deepwater Drilling and Completions Conference. Society of Petroleum Engineers.

Evje, S. and Fjelde, K.K., 2002. Hybrid flux-splitting schemes for a two-phase flow model. Journal of Computational Physics, 175(2): 674-701.

Gate energy, 2015. Well integrity: A holistic approach to annulus pressure management for subsea wells. Retrieved from https://www.gateinc.com/gatekeeper/gat2004-gkp-2015-09.

Halal, A.S. and Mitchell, R., 1994. Casing design for trapped annular pressure buildup. SPE Drilling & Completion, 9(02): 107-114.

Hasan, A. and Kabir, C., 2012. Wellbore heat-transfer modeling and applications. Journal of Petroleum Science and Engineering, 86: 127-136.

Hasan, A.R., Kabir, C.S. and Sarica, C., 2002. Fluid flow and heat transfer in wellbores. Society of Petroleum Engineers Richardson, TX.

Hasan, R., Izgec, B. and Kabir, S., 2010. Sustaining Production by Managing Annular-Pressure Buildup.

Hewitt, G.F. and Hall-Taylor, N.S., 1970. Annular Two-phase Flow. Pergamon Press, Oxford ; New York.

Jandhyala, S.R.K. and Chiney, A., 2014. Finite element approach to predict the effect of annular pressure buildup on wellbore materials, Offshore Technology Conference-Asia. Offshore Technology Conference.

Jin, Y., Haixiong, T., Zhengli, L., Liping, Y., Huang, X., De, Y. and Ruirui, T., 2013. Prediction model of casing annulus pressure for deepwater well drilling and completion operation. Petroleum Exploration and Development, 40(5): 661-664.

Kanev, K., Ikeuchi, J., Kimurat, S. and Okajima, A., 1997. Heat loss to the surrounding rock formation from a geothermal wellbore. Geothermics, 26(3): 329-349.

Liu, Z., Samuel, R., Gonzales, A. and Kang, Y., 2016. Modeling and Simulation of Annular Pressure Buildup APB Management Using Syntactic Foam in HP/HT Deepwater Wells, SPE Deepwater Drilling and Completions Conference. Society of Petroleum Engineers.

MacEachran, A. and Adams, A.I., 1991. Impact on Casing Design of Thermal Expansion of Fluids in Confined Annuli. Paper SPE 21911 presented at the 1991 speliadc drilling conference, Amsterdam.

Mitchell, R. and Wedelich III, H., 1989. Prediction of downhole temperatures can be key for optimal wellbore design, SPE Production Operations Symposium. Society of Petroleum Engineers.

Moe, B. and Erpelding, P., 2000. Annular pressure buildup: What it is and what to do about it. World Oil, 221(8): 21-23.

Movahedi, H., Shad, S. and Mokhtari-Hosseini, Z.B., 2018. Modeling and simulation of barite deposition in an annulus space of a well using CFD. Journal of Petroleum Science and Engineering, 161: 476-496.

Norsok Standard D-010, 2013. Well integrity in drilling and well operations, Rev. 4. The Norwegian Oil Industry Association, Lysaker, Norway.

Oudeman, P. and Bacarreza, L., 1995. Field trial results of annular pressure behavior in a high-pressure/high-temperature well. SPE Drilling & Completion, 10(02): 84-88.

Oudeman, P. and Kerem, M., 2006. Transient behavior of annular pressure build-up in HP/HT wells. SPE Drilling & Completion, 21(04): 234-241.

Pattillo, P.D., Cocales, B.W. and Morey, S.C., 2004. Analysis of an Annular Pressure Buildup Failure during Drill Ahead, SPE Annual Technical Conference and Exhibition. Society of Petroleum Engineers, Houston, Texas.

Pauchon, C. and Dhulesia, H., 1994. TACITE: A transient tool for multiphase pipeline and well simulation, SPE Annual Technical Conference and Exhibition. Society of Petroleum Engineers.

Perdana, T.P.A. and Zulkhifly, S., 2015. Annular Pressure Build Up in Subsea Well, in the Proceedings of Indonesian Petroleum Association, Thirty-Ninth Annual Convention & Exhibition, Indonesia.

Petersen, J., Rommetveit, R., Bjorkevoll, K.S. and Froyen, J., 2008. A general dynamic model for single and multi-phase flow operations during drilling, completion, well control and intervention, IADC/SPE Asia Pacific Drilling Technology Conference and Exhibition. Society of Petroleum Engineers.

Ramey Jr, H., 1962. Wellbore heat transmission. Journal of petroleum Technology, 14(04): 427-435.

Sathuvalli, U., Pilko, R., Gonzalez, R., Pai, R., Sachdeva, P. and Suryanarayana, P., 2016. Design and performance of annular pressure build-up (APB) mitigation techniques, IADC/SPE Drilling Conference and Exhibition. Society of Petroleum Engineers.

Sorelle, R.R., Jardiolin, R.A., Buckley, P. and Barrios, J.R., 1982. Mathematical field model predicts downhole density changes in static drilling fluids, SPE Annual Technical Conference and Exhibition. Society of Petroleum Engineers.

Stamnes, Ø.N., 2011. Nonlinear Estimation with Applications to Drilling, Norwegian University of Science and Technology (NTNU), Norway.

Taitel, Y., Bornea, D. and Dukler, A., 1980. Modelling flow pattern transitions for steady upward gas-liquid flow in vertical tubes. AIChE Journal, 26(3): 345-354.

Udegbunam, J.E., Fjelde, K.K., Evje, S. and Nygaard, G., 2015. On the advection-upstream-splitting-method hybrid scheme: a simple transient-flow model for managed-pressure-drilling and underbalanced-drilling applications. SPE Drilling & Completion, 30(02): 98-109.

Udegbunam, J.E., Sui, D., Moeinikia, F., Lage, A.C., Fjelde, K.K., Arild, Ø., Rabenjafimanantsoa, H.A. and Nygaard, G.H., 2017. A Transient Flow Model for Predicting Pressure Buildup in Closed Annuli, ASME 2017 36th International Conference on Ocean, Offshore and Arctic Engineering. American Society of Mechanical Engineers, pp. V008T11A028-V008T11A028.

Vargo Jr, R.F., Payne, M., Faul, R., LeBlanc, J. and Griffith, J.E., 2003. Practical and successful prevention of annular pressure buildup on the Marlin project. SPE drilling & completion, 18(03): 228-234.

Wallis, G.B., 1969. One-dimensional two-phase flow. McGraw-Hill, Inc., New York.

Williamson, R., Sanders, W., Jakabosky, T., Serio, M. and Griffith, J.E., 2003. Control of contained-annulus fluid pressure buildup, SPE/IADC Drilling Conference. Society of Petroleum Engineers.

Yin, F. and Gao, D., 2014. Improved calculation of multiple annuli pressure buildup in subsea HPHT wells, IADC/SPE Asia Pacific Drilling Technology Conference. Society of Petroleum Engineers.

Zhou, F. and Zheng, X., 2015. Heat transfer in tubing-casing annulus during production process of geothermal systems. Journal of Earth Science, 26(1): 116-123.

Zhu, W., 2003. An Investigation of Two-Phase Flow Regime Transition in Large Diameter Pipes (master's thesis), McMaster University, Hamilton, Ontario.

Appendix: AUSMV Matlab code

```
% Transient two-phase code based on AUSMV scheme: Barite and Water
% The code assumes uniform geometry and the code is partially vectorized.

% Overview of main physical parameters. All these are defined as vectors
% reflecting the cells in the discretization. Note that all variables are
% defined in the midpoint of the cells.

%  time - seconds
%
% p - pressure at new timelevel (Pa)
% dl - density of liquid at new timelevel (kg/m3)
% dg - density of barite at new timelevel (kg/m3)
% eg - phase volume fraction of barite [0-1]
% ev - phase volume fraction of water [0-1]. eg+el =1
% vg - phase velocity of barite (m/s). Negative value is downward movement.
% vl - phase velocity of water (m/s)
% qv - conservative variables at new timelevel
% temp - temperature in annulus at new time  (Kelvin).

% po - pressure at new timelevel (Pa)
% dlo - density of liquid at new timelevel (kg/m3)
% dgo - density of barite at new timelevel (kg/m3)
% ego - phase volume fraction of barite [0-1]
% evo - phase volume fraction of water [0-1]. eg+el =1
% vg - phase velocity of barite (m/s). Negative value is downward movement.
% vl - phase velocity of water (m/s)
% qvo - conservative variables at new timelevel
% tempo - temperature in annulus at time = 0. The initial temperature
% (Kelvin)

% At each timelevel, the numerical scheme will update the conservative
% variables and we have to find the physical variables using the
% conservative variable values in combination with the density models and
% the slip relation.


clear;
t = cputime
tic,

% Geometry data/ Must be specified
welldepth = 4000;  % Vertical depth/length of A annulus (meters)
nobox = 25; %Number of boxes in the well
nofluxes = nobox+1;
dx = welldepth/nobox; % Boxlength (meters)
%dt = 0.005;

% Welldepth array for plotting
x(1)= -1.0*welldepth+0.5*dx;
for i=1:nobox-1
 x(i+1)=x(i)+ dx;
```

```
end

dt= 0.02;  % Timestep   Note that this must satisfy cfl condition:
% dt < (cfl x dx )/speed of sound in water. CFL is a number: 0 < cfl < 1
dtdx = dt/dx;
time = 0.0; % Start time for simulation
endtime = 1900; % End time for simulation
nosteps = endtime/dt;  %Number of total timesteps
timebetweensavingtimedata = 5;  % How often in s we save data vs time for
plotting.
nostepsbeforesavingtimedata = timebetweensavingtimedata/dt;

% Slip parameters used in the gas slip relation. vg =Kvmix+S. Modified
% later in code
k = 1.0;
s =0;
pbondout=10000000;  % Initial pressure on top of annulus, assume 1000 meter
water depth

% Initial temperature distribution.

tempbot = 120+273; % Temperature at bottom of A annulus
temptop = 4+273;  % Temperature at top of A annulus. We start out with a
temperature profile
% equal to geothermal gradient
tempgrad= (tempbot-temptop)/welldepth;
tempo(1)=tempbot-dx/2*tempgrad;
for i = 1:nobox-2
  tempo(i+1)=tempo(i)-dx*tempgrad;
end
tempo(nobox)=tempo(nobox-1)-dx*tempgrad;

% Here we specify what the final temperatures shall be when production has
% heated up the annuli
tempbotfinal = 120+273;
temptopfinal = 60+273;
tempgradfinal= (tempbotfinal-temptopfinal)/welldepth;
tempfinal(1)=tempbotfinal-dx/2*tempgradfinal;
for i = 1:nobox-2
  tempfinal(i+1)=tempfinal(i)-dx*tempgradfinal;
end
tempfinal(nobox)=tempfinal(nobox-1)-dx*tempgradfinal;

% Here we specify the timeperiod for builduptemperature
timeperiod = 1000;  %Normally it takes much longer time. We speed up the
process in the simulation

% Here we specify how the temperature changes vs time for the different
% cells. Note that we must do it like this since the build up is different
% in the different cells.
for i = 1:nobox
   tempbuilduptimegradient(i) = (tempfinal(i)-tempo(i))/timeperiod;
end
```

```
% Fluid parameters
rho0=1000;    % Water density at STC
P0=100000;    % Pressure at STC (Pa)
Bheta=2.2*10^9;  % Parameterer reflecting compressibility of liquid related
to pressure
Alpha=0.000207;  % Parameterer reflecting compressibility of liquid related
to temperatuer
T0=20+273.15;  % Temperature at STC
baritedensity = 4200  % kg/m3
al = 1500; % Speed of sound in water.




% Viscosities (Pa*s)/Used in the frictional pressure loss model.
viscl = 0.001; % Liquid phase
viscg = 0.001; % Barite phase. We just approximate the viscosity of the
mixture to be
% equal to viscosity of water


% Gravity constant

  g = 9.81; % Gravitational constant

% Well opening. opening = 1, fully open well, opening = 0 (<0.01), the well
% is fully closed. This variable will control what boundary conditions that
% will apply at the outlet (both physical and numerical): We must change
% this further below in the code if we want to change status on this.

  wellopening = 1.0;  % This variable determines if
%the well is closed or not, wellopening = 1.0 -> open. welllopening = 0
%-> Well is closed. This variable affects the boundary treatment.

  bullheading = 0.0; % This variable can be set to 1.0 if we want to simulate
% a bullheading operation. But the normal is to set this to zero.


% Specify if the primitive variables shall be found either by
% a numerical or analytical approach. If analytical = 1, analytical
% solution is used. If analytical = 0. The numerical approach is used.
% using the itsolver subroutine where the bisection numerical method
% is used.

  analytical = 1;


% Define and intilalize flow variables
```

```
% Here we specify the outer and inner diameter and the flow area
% Note that one of the adjustments we are going to make is to change this
% geometry as function of pressure. But here it is only initialized.


% Geometry assumed. Inner diameter is a 7 inch production tubing.
% Outer dimater is inner diameter of a 9 5/8 inch production casing.
   for i = 1:nobox

    do(i)=0.21662;
    di(i) = 0.1778;
    area(i) = 3.14/4*(do(i)*do(i)- di(i)*di(i));

   end




% Initialization of slope limiters. These are used to make the numerical
% scheme second order and more accurate, not needing so many numerical
% cells to obtain a good solution.

  for i = 1:nobox
    sl1(i)=0;
    sl2(i)=0;
    sl3(i)=0;
    sl4(i)=0;
    sl5(i)=0;
    sl6(i)=0;
  end



% Now comes the intialization of the physical variables in the well.
% First primitive variables, then the conservative ones.




% Below we intialize pressure and fluid densities. We start from top of
% the well and calculated downwards. The calculation is done twice with
% updated values to get better approximation. Only hydrostatic
% considerations.

for i = 1:nobox
  eg(i)=0.2;  % Barite volume fraction. 20 %
  ev(i)=1-eg(i); % Liquid volume fraction
end
```

```
p(nobox)= pbondout+0.5*g*dx*(ev(nobox)*rho0+eg(nobox)*baritedensity);    %
Pressure
dl(nobox)=rholiq(p(nobox),tempo(nobox));  % Liquid density
dg(nobox)=rogas(p(nobox));    % Gas density




for i=nobox-1:-1:1
p(i)=p(i+1)+dx*g*(ev(i+1)*dl(i+1)+eg(i+1)*dg(i+1));
dl(i)=rholiq(p(i),tempo(i));
dg(i)=rogas(p(i));
end

 for i=nobox-1:-1:1
  rhoavg1= (ev(i+1)*dl(i+1)+eg(i+1)*dg(i+1))
  rhoavg2= (ev(i)*dl(i)+eg(i)*dg(i))
  p(i)=p(i+1)+dx*g*(rhoavg1+rhoavg2)*0.5;
  dl(i)=rholiq(p(i),tempo(i));
  dg(i)=rogas(p(i));

 end

% Intitialize phase velocities, volume fractions, conservative variables
% The basic assumption is static fluid, one phase liquid.

for i = 1:nobox
  vl(i)=0; % Liquid velocity new time level.
  vg(i)=0; % Gas velocity at new time level
  qv(i,1)=dl(i)*ev(i)*area(i);
  qv(i,2)=dg(i)*eg(i)*area(i);
  qv(i,3)=(dl(i)*ev(i)*vl(i)+dg(i)*eg(i)*vg(i))*area(i);
  fricgrad(i)=0;
  hydgrad(i)=g*(dl(i)*ev(i)+eg(i)*dg(i));
end

source = zeros(nobox,3);


% Section where we also initialize values at old time level


for i=1:nobox
  dlo(i)=dl(i);
  dgo(i)=dg(i);
  po(i)=p(i);
  ego(i)=eg(i);
  evo(i)=ev(i);
  vlo(i)=vl(i);
  vgo(i)=vg(i);
  qvo(i,1)=qv(i,1);
  qvo(i,2)=qv(i,2);
  qvo(i,3)=qv(i,3);
end
```

```
% ALL VARIABLES ARE NOW INITIALIZED


% Intialize fluxes between the cells/boxes

for i = 1:nofluxes
  for j =1:3
   flc(i,j)=0.0; % Flux of liquid over box boundary
   fgc(i,j)=0.0; % Flux of gas over box boundary
   fp(i,j)= 0.0; % Pressure flux over box boundary
  end
end


%  Main program. Here we will progress in time. First som intializations
% and definitions to take out results. The for loop below runs until the
% simulation is finished.

countsteps = 0;
counter=0;
printcounter = 1;
pin(printcounter) = (p(1)+dx*0.5*hydgrad(1))/100000;
pout(printcounter)= pbondout/100000;
pnobox(printcounter)= p(nobox)/100000;
liquidmassrateout(printcounter) = 0;
gasmassrateout(printcounter)=0;
timeplot(printcounter)=time;
kickvolume=0;
bullvolume=0;


% The following for loop advanced the simulation timestep by timestep
% forward in time
for i = 1:nosteps
   countsteps=countsteps+1;
   counter=counter+1;
   time = time+dt;

%  Here we can define the S parameter to simulate that barite falls
downwards.
%  We start by just assuming S = 0 (K = 1 from before). This will ensure
%  that no settling of barite takes place. Suggest that we only look at
%  effect of temperature and then geometry change first.

  if (time<30)
  timeint=(time)/30;
%  s=-0.5*timeint;
  s=0;
  else
%  s=-0.5;
  s=0;

  end
```

```
% Then a section where specify the boundary conditions.
% Here we specify the inlet rates of the different phases at the
% bottom of the pipe in kg/s. We interpolate to make things smooth.
% It is also possible to change the outlet boundary status of the well
% here (open and closed). We always start with an open geometry.
% This is a place where we can change the
% code to control simulations.




XX= 0;   % Inlet rates at bottom are zero since we have a annulus with
stagnant liquid + barite
YY= 0;

if (time<100)
  inletligmassrate=0.0;
  inletgasmassrate=0.0;
else
  inletligmassrate=0.0;
  inletgasmassrate=0.0;
  wellopening=0;   % After 100 seconds we close the annulus!
end

% Below we control the temperature development. Start to heat the annulus
% after 100 seconds

if (time<=100)
  for ii = 1:nobox
    temp(ii)=tempo(ii);  % no heating the first 100 seconds
  end
else
  for ii = 1:nobox
    temp(ii)=tempo(ii)+(time-100)*tempbilduptimegradient(ii);
  end
end

%  HERE WE IMPLEMENNTING THE AREA CHANGE IN TIME.
%  WE JUST ASSUME THAT THE AREA CHANGE IS TIME DEPENDENT USING SIMPLE
%  INTERPOLATION TECHNIQUE.
%

for j = 1:nobox
    if (time<=100)
        area(j) = area(j);
    else
        do(j) = 0.21662+((time-100)/(endtime-100))*0.0001;
        di(j) = 0.1778-((time-100)/(endtime-100))*0.0001;
        area(j) = 3.14/4*(do(j)*do(j)- di(j)*di(j));

    end
end
```

```
% specify the outlet pressure /Physical. Here we have given the pressure as
% constant. It would be possible to adjust it during openwell conditions
% either by giving the wanted pressure directly (in the command lines
% above) or by finding it indirectly through a chokemodel where the
wellopening
% would be an input parameter. The wellopening variable would equally had
% to be adjusted inside the command line structure given right above.

 pressureoutlet = pbondout;

% Based on these boundary values combined with use of extrapolations
techniques
% for the remaining unknowns at the boundaries, we will define the mass and
% momentum fluxes at the boundaries (inlet and outlet of pipe).

% inlet/bottom fluxes first.
   if (bullheading<=0)

     flc(1,1)= inletligmassrate/area(1);
     flc(1,2)= 0.0;
     flc(1,3)= flc(1,1)*vlo(1);


     fgc(1,1)= 0.0;
     fgc(1,2)= inletgasmassrate/area(1);
     fgc(1,3)= fgc(1,2)*vgo(1);

     fp(1,1)= 0.0;
     fp(1,2)= 0.0;

% Old way of treating the boundary
%     fp(1,3)= po(1)+0.5*(po(1)-po(2)); %Interpolation used to find the
% pressure at the inlet/bottom of the well.

% New way of treating the boundary
      fp(1,3)= po(1)...
            +0.5*dx*(dlo(1)*evo(1)+dgo(1)*ego(1))*g...
            +0.5*dx*fricgrad(1);



   else
     flc(1,1)=dlo(1)*evo(1)*vlo(1);
     flc(1,2)=0.0;
     flc(1,3)=flc(1,1)*vlo(1);

     fgc(1,1)=0.0;
     fgc(1,2)=dgo(1)*ego(1)*vgo(1);
     fgc(1,3)=fgc(1,2)*vgo(1);

     fp(1,1)=0.0;
     fp(1,2)=0.0;
```

```
     fp(1,3)=20000000; % This was a fixed pressure set at bottom when
bullheading
   end




% Outlet fluxes (open & closed conditions)

    if (wellopening>0.01)

% Here open end condtions are given. We distinguish between bullheading
% & normal circulation.

        if (bullheading<=0)

            pakk1=dlo(nobox)*evo(nobox)*vlo(nobox);
            pakk2=dlo(nobox-1)*evo(nobox-1)*vlo(nobox-1);
            diff=pakk2-pakk1;
            diff=0;


            flc(nofluxes,1)= dlo(nobox)*evo(nobox)*vlo(nobox)-0.5*diff;
            flc(nofluxes,2)= 0.0;

            diff=vlo(nobox-1)-vlo(nobox);
            diff=0;
            flc(nofluxes,3)= flc(nofluxes,1)*(vlo(nobox)+0.5*diff);


            pakk1=dgo(nobox)*ego(nobox)*vgo(nobox);
            pakk2=dgo(nobox-1)*ego(nobox-1)*vgo(nobox-1);
            diff=pakk2-pakk1;
            diff = 0;

            fgc(nofluxes,1)= 0.0;
            fgc(nofluxes,2)= dgo(nobox)*ego(nobox)*vgo(nobox)-0.5*diff;
            fgc(nofluxes,3)= fgc(nofluxes,2)*vgo(nobox);

            fp(nofluxes,1)= 0.0;
            fp(nofluxes,2)= 0.0;
            fp(nofluxes,3)= pressureoutlet;
        else
            flc(nofluxes,1)= inletligmassrate/area(nobox);
            flc(nofluxes,2)= 0.0;
            flc(nofluxes,3)= flc(nofluxes,1)*vlo(nobox);

            fgc(nofluxes,1)=0.0;
            fgc(nofluxes,2)=0.0;
            fgc(nofluxes,3)=0.0;

            fp(nofluxes,1)=0.0;
            fp(nofluxes,2)=0.0;
```

```
            fp(nofluxes,3)= po(nobox)...
            -0.5*dx*(dlo(nobox)*evo(nobox)+dgo(nobox)*ego(nobox))*g...
            +0.5*dx*fricgrad(nobox);
        end
    else

% Here closed end conditions are given

         flc(nofluxes,1)= 0.0;
         flc(nofluxes,2)= 0.0;
         flc(nofluxes,3)= 0.0;

         fgc(nofluxes,1)= 0.0;
         fgc(nofluxes,2)= 0.0;
         fgc(nofluxes,3)= 0.0;

         fp(nofluxes,1)=0.0;
         fp(nofluxes,2)=0.0;

    %    Old way of treating the boundary
    %     fp(nofluxes,3)= po(nobox)-0.5*(po(nobox-1)-po(nobox));

    %    New way of treating the boundary
         fp(nofluxes,3)= po(nobox)...
         -0.5*dx*(dlo(nobox)*evo(nobox)+dgo(nobox)*ego(nobox))*g;
    %     -0.5*dx*fricgrad(nobox); % Neglect friction since well is closed.
        end


 % Implementation of slopelimiters. They are applied on the physical
 % variables like phase densities, phase velocities and pressure.



     for i=2:nobox-1
      sl1(i)=minmod(dlo(i-1),dlo(i),dlo(i+1),dx);
      sl2(i)=minmod(po(i-1),po(i),po(i+1),dx);
      sl3(i)=minmod(vlo(i-1),vlo(i),vlo(i+1),dx);
      sl4(i)=minmod(vgo(i-1),vgo(i),vgo(i+1),dx);
      sl5(i)=minmod(ego(i-1),ego(i),ego(i+1),dx);
      sl6(i)=minmod(dgo(i-1),dgo(i),dgo(i+1),dx);
     end

 % TWO ALTERNATIVES ARE SHOWN BELOW FOR HOW TO FIND THE SLOPES IN THE
BOUNDARY CELLS

 % Slopelimiters in boundary cells are set to zero!
     sl1(nobox)=0;
     sl2(nobox)=0;
     sl3(nobox)=0;
     sl4(nobox)=0;
     sl5(nobox)=0;
     sl6(nobox)=0;
```

```
  % Slopelimiters in boundary cells are copied from neighbour box!
     sl1(nobox)=sl1(nobox-1);
     sl2(nobox)=sl2(nobox-1);
     sl3(nobox)=sl3(nobox-1);
     sl4(nobox)=sl4(nobox-1);
     sl5(nobox)=sl5(nobox-1);
     sl6(nobox)=sl6(nobox-1);

   % Slopelimiters in boundary cells are set to zero!
     sl1(1)=0;
     sl2(1)=0;
     sl3(1)=0;
     sl4(1)=0;
     sl5(1)=0;
     sl6(1)=0;

   % Slopelimiters in boundary cells are copied from neighbour box!
     sl1(1)=sl1(2);
     sl2(1)=sl2(2);
     sl3(1)=sl3(2);
     sl4(1)=sl4(2);
     sl5(1)=sl5(2);
     sl6(1)=sl6(2);


% Now we will find the fluxes between the different cells.
% NB - IMPORTANE -  Note that if we change the compressibilities/sound
velocities of
% the fluids involved, we need to do changes inside the csound function.

     for j = 2:nofluxes-1

 %%%%%%%%%%%%%%%%%%%%%%%%%%%%%%%%%%%%%%%%%%%%%%%
 %%%%%%%%%%%%%%%%%%%%%%%%%%%%%%%%%%%%%%%%%%%%%%%
 % First order method is from here:
%         cl = csound(ego(j-1),po(j-1),dlo(j-1),k);
%         cr = csound(ego(j),po(j),dlo(j),k);
%         c = max(cl,cr);
%         pll = psip(vlo(j-1),c,evo(j));
%         plr = psim(vlo(j),c,evo(j-1));
%         pgl = psip(vgo(j-1),c,ego(j));
%         pgr = psim(vgo(j),c,ego(j-1));
%         vmixr = vlo(j)*evo(j)+vgo(j)*ego(j);
%         vmixl = vlo(j-1)*evo(j-1)+vgo(j-1)*ego(j-1);
%
%         pl = pp(vmixl,c);
%         pr = pm(vmixr,c);
%         mll= evo(j-1)*dlo(j-1);
%         mlr= evo(j)*dlo(j);
%         mgl= ego(j-1)*dgo(j-1);
%         mgr= ego(j)*dgo(j);
%
%         flc(j,1)= mll*pll+mlr*plr;
%         flc(j,2)= 0.0;
%         flc(j,3)= mll*pll*vlo(j-1)+mlr*plr*vlo(j);
%
```

```
%         fgc(j,1)=0.0;
%         fgc(j,2)= mgl*pgl+mgr*pgr;
%         fgc(j,3)= mgl*pgl*vgo(j-1)+mgr*pgr*vgo(j);
%
%         fp(j,1)= 0.0;
%         fp(j,2)= 0.0;
%         fp(j,3)= pl*po(j-1)+pr*po(j);

 %  First order methods ends here
 %%%%%%%%%%%%%%%%%%%%%%%%%%%%%%%%%%%%%%%%%%%%%%%%%%%%%%%
 %%%%%%%%%%%%%%%%%%%%%%%%%%%%%%%%%%%%%%%%%%%%%%%%%%%%%%%%%




%%%%%%%%%%%%%%%%%%%%%%%%%%%%%%%%%%%%%%%%%%%%%%%%%%%%%%%%%%
%%%%%%%%%%%%%%%%%%%%%%%%%%%%%%%%%%%%%%%%%%%%%%%%%%%%%%%%%%
% Second order method starts here:
% Here slopelimiter is used on all variables except phase velocoties

       psll = po(j-1)+dx/2*sl2(j-1);
       pslr = po(j)-dx/2*sl2(j);
       dsll = dlo(j-1)+dx/2*sl1(j-1);
       dslr = dlo(j)-dx/2*sl1(j);
       dgll = dgo(j-1)+dx/2*sl6(j-1);
       dglr = dgo(j)-dx/2*sl6(j);

       vlv = vlo(j-1)+dx/2*sl3(j-1);
       vlh = vlo(j)-dx/2*sl3(j);
       vgv = vgo(j-1)+dx/2*sl4(j-1);
       vgh = vgo(j)-dx/2*sl4(j);

       gvv = ego(j-1)+dx/2*sl5(j-1);
       gvh = ego(j)-dx/2*sl5(j);
       lvv = 1-gvv;
       lvh = 1-gvh;

       cl = csound(gvv,psll,dsll,k);
       cr = csound(gvh,pslr,dslr,k);
       c = max(cl,cr);

       pll = psip(vlo(j-1),c,lvh);
       plr = psim(vlo(j),c,lvv);
       pgl = psip(vgo(j-1),c,gvh);
       pgr = psim(vgo(j),c,gvv);
       vmixr = vlo(j)*lvh+vgo(j)*gvh;
       vmixl = vlo(j-1)*lvv+vgo(j-1)*gvv;

       pl = pp(vmixl,c);
       pr = pm(vmixr,c);


      mll= lvv*dsll;
      mlr= lvh*dslr;
```

```
      mgl= gvv*dgll;
      mgr= gvh*dglr;

      flc(j,1)= mll*pll+mlr*plr;
      flc(j,2)= 0.0;
      flc(j,3)= mll*pll*vlo(j-1)+mlr*plr*vlo(j);


      fgc(j,1)=0.0;
      fgc(j,2)= mgl*pgl+mgr*pgr;
      fgc(j,3)= mgl*pgl*vgo(j-1)+mgr*pgr*vgo(j);

      fp(j,1)= 0.0;
      fp(j,2)= 0.0;
      fp(j,3)= pl*psll+pr*pslr;

 % Brute force on mass fluxes. We dont allow the sediment concentration to
 % exceed 0.5. This was the only way to fix this problem by forcing the
 % fluxes to zero.

      if(eg(j-1)>=0.5)
        fgc(j,2)=0;
        fgc(j,3)=0;
      end

     end

% Fluxes have now been calculated. We will now update the conservative
% variables in each of the numerical cells.

% Here we calcualte the source terms (friction and hydrostatic pressure
% gradients in the momentum equation
% Note that the model is sensitive to how we treat the model
% for low Reynolds numbers (possible discontinuty in the model)

       for j=1:nobox
        fricgrad(j)=dpfric(vlo(j),vgo(j),evo(j),ego(j),dlo(j),dgo(j), ...
          po(j),do(j),di(j),viscl,viscg);
        hydgrad(j)=g*(dlo(j)*evo(j)+dgo(j)*ego(j));
       end

      sumfric = 0;
      sumhyd= 0;

      for j=1:nobox
%  Here we update the conservative variables in all cells at the new
timelevel
%  based on values from the old timelevel.

%
% NBNBNB - HERE WE SEE GEOMETRY BEING USED IN THE CONSERVATION LAWS. THIS
% MUST BE ALLOWED TO CHANGE
       ar = area(j);
%
```

```
      qv(j,1)=qvo(j,1)-dtdx*((ar*flc(j+1,1)-ar*flc(j,1))...
                            +(ar*fgc(j+1,1)-ar*fgc(j,1))...
                            +(ar*fp(j+1,1)-ar*fp(j,1)));

      qv(j,2)=qvo(j,2)-dtdx*((ar*flc(j+1,2)-ar*flc(j,2))...
                            +(ar*fgc(j+1,2)-ar*fgc(j,2))...
                            +(ar*fp(j+1,2)-ar*fp(j,2)));

      qv(j,3)=qvo(j,3)-dtdx*((ar*flc(j+1,3)-ar*flc(j,3))...
                            +(ar*fgc(j+1,3)-ar*fgc(j,3))...
                            +(ar*fp(j+1,3)-ar*fp(j,3)))...
                  -dt*ar*(fricgrad(j)+hydgrad(j));

%
      sumfric=sumfric+fricgrad(j)*dx;
      sumhyd=sumhyd+hydgrad(j)*dx;

      end




% Section where we find the physical variables (pressures, densities etc)
% from the conservative variables. Some trickes to ensure stability. These
% are induced to avoid negative masses.



     gasmass=0;
     liqmass=0;

     for j=1:nobox


% Remove the area from the conservative variables to find the
% the primitive variables from the conservative ones.

% NBNBNB - HERE WE SEE GEOMETRY BEING USED IN THE CONSERVATION LAWS. THIS
% MUST BE ALLOWED TO CHANGE

      qv(j,1)= qv(j,1)/area(j);
      qv(j,2)= qv(j,2)/area(j);

      if (qv(j,1)<0.00000001)
        qv(j,1)=0.00000001;
      end

      if (qv(j,2)< 0.00000001)
        qv(j,2)=0.00000001;
      end
```

```
      gasmass = gasmass+qv(j,2)*area(j)*dx;
      liqmass = liqmass+qv(j,1)*area(j)*dx;

% Below, we find the primitive variables pressure and densities based on
% the conservative variables q1,q2. One can choose between getting them by
% analytical or numerical solution approach specified in the beginning of
% the program. Ps. For more advanced density models, this must be changed.


      if (analytical == 1)
          eg(j)= qv(j,2)/baritedensity;
          ev(j)=1-eg(j);
          dg(j)=baritedensity;
          if (ev(j)>0.01)
            dl(j)=qv(j,1)/ev(j);
            h11=dl(j)-rho0+rho0*Alpha*(temp(j)-T0);
            p(j)=P0+Bheta/rho0*h11;
          else
            dl(j)=qv(j,1)/0.001;
            h11=dl(j)-rho0+rho0*Alpha*(temp(j)-T0);
            p(j)=P0+Bheta/rho0*h11;
          end

      else
      %Numerical Solution: Not used
       [p(j),error]=itsolver(po(j),qv(j,1),qv(j,2)); % Pressure
       dl(j)=rholiq(p(j),temp(j)); % Density of liquid
       dg(j)=rogas(p(j)); % Density of gas

      % Incase a numerical solution is not found, the program will write out
"error":
       if error > 0
          error
       end
      end

%   Find Volume fractions
% %       eg(j)= qv(j,2)/dg(j);
% %       ev(j)=1-eg(j);

 %     Reset average conservative varibles in cells with area changes inside.

     qv(j,1)=qv(j,1)*area(j);
     qv(j,2)=qv(j,2)*area(j);

     end  % end of loop
```

```
 %    Below we find the phase velcoties by combining the
 %    conservative variable defined by the mixture momentum equation q3
 %    with the gas slip relation.
 %    At the same time we try to summarize the gas (in this case barite)
volume in the well.


   gasvol=0;

   for j=1:nobox


   % The interpolations introduced below are included
   % to omit a singularity in the slip relation when the gas volume
   % fraction becomes equal to 1/K. In additon, S is interpolated to
   % zero when approaching one phase gas flow. In the transition to
   % one phase gas flow, we have no slip condtions (K=1, S=0)

      ktemp=k;
      stemp=s;

      k0(j) = ktemp;
      s0(j) = stemp;
      if ((eg(j)>=0.7) & (eg(j)<=0.8))
        xint = (eg(j)-0.7)/0.1;
        k0(j) =1.0*xint+k*(1-xint);
      elseif(eg(j)>0.8)
        k0(j)=1.0;
      end

%       if ((eg(j)>=0.9) & (eg(j)<=1.0))
%         xint = (eg(j)-0.9)/0.1;
%         s0(j) = 0.0*xint+s*(1-xint);
%       end

      if ((eg(j)>=0.3) & (eg(j)<=0.5))
        xint = (eg(j)-0.3)/0.2;
        s0(j) = 0.0*xint+s*(1-xint);
      elseif(eg(j)>0.5)
        s0(j) = 0.0;
      end

      if (eg(j)>=0.999999)
        k1(j) = 1.0;
        s1(j) = 0.0;
      else
        k1(j) = (1-k0(j)*eg(j))/(1-eg(j));
        s1(j) = -1.0*s0(j)*eg(j)/(1-eg(j));
      end

      help1 = dl(j)*ev(j)*k1+dg(j)*eg(j)*k0;
      help2 = dl(j)*ev(j)*s1+dg(j)*eg(j)*s0;
```

```
      vmixhelpl = (qv(j,3)/area(j)-help2)/help1;
      vg(j)=k0(j)*vmixhelpl+s0(j);
      vl(j)=k1(j)*vmixhelpl+s1(j);

      % Variable for summarizing the gas volume content in the well.
      gasvol=gasvol+eg(j)*area(j)*dx;


   end


% Old values are now set equal to new values in order to prepare
% computation of next time level.


   po=p;
   dlo=dl;
   dgo=dg;
   vlo=vl;
   vgo=vg;
   ego=eg;
   evo=ev;
   qvo=qv;




% Section where we save some timedependent variables in arrays.
% e.g. the bottomhole pressure. They will be saved for certain
% timeintervalls defined in the start of the program in order to ensure
% that the arrays do not get to long!

  if (counter>=nostepsbeforesavingtimedata)
    printcounter=printcounter+1;
    time

    % Outlet massrates vs time

liquidmassrateout(printcounter)=dl(nobox)*ev(nobox)*vl(nobox)*area(nobox);
%Water kg/s
    gasmassrateout(printcounter)=dg(nobox)*eg(nobox)*vg(nobox)*area(nobox);
% Barite kg/s

    % Hydrostatic and friction pressure in well vs time in bar
    hyd(printcounter)=sumhyd/100000;
    fric(printcounter)=sumfric/100000;

    % Volume of barite in well vs time (m3)

    volgas(printcounter)=gasvol;

    % Total phase masses in the well vs time  (kg)
```

```
    massgas(printcounter)=gasmass; % Barite
    massliq(printcounter)=liqmass; % Water


    % pout defines the exact pressure at the top of A annulus.
    % Note that 0.5 comes from the fact that the pressure we want to plot
    % is the pressure at the boundaries of the cells. Remember the physical
    % variables are defined in the mid of cells.

    pout(printcounter)=(p(nobox)-0.5*dx*...
    (dlo(nobox)*evo(nobox)+dgo(nobox)*ego(nobox))*g-
dx*0.5*fricgrad(nobox))/100000;
    % pin defines the exact pressure at the bottom of A annulus
    pin(printcounter)=
(p(1)+0.5*dx*(dlo(1)*evo(1)+dgo(1)*ego(1))*g+0.5*dx*fricgrad(1))/100000;

    pnobox(printcounter)=p(nobox)/100000 % just printing pressure in topbox
to screen to check it is
    % increasing.

    % Time variable
    timeplot(printcounter)=time;  % vector that contain time for plotting

    counter = 0;


  end
end    % LOOP THAT RUNS FORWARD IN TIME

% end of stepping forward in time.




% Printing of resultssection


countsteps % Marks number of simulation steps.


% Plot commands for variables vs time. The commands can also
% be copied to command screen where program is run for plotting other
% variables.

toc,
e = cputime-t

% Plot bottomhole pressure
plot(timeplot,pin)

% Plot pressure at top of annulus.
%plot(timeplot,pout)
```

```
% Show cfl number used.
disp('cfl')
cfl = al*dt/dx

% Some other possible plotting possibilies.

%plot(timeplot,liquidmassrateout)
%plot(timeplot,gasmassrateout)

%Plot commands for variables vs depth/Only the last simulated
%values at endtime is visualised

%plot(vl,x);
%plot(vg,x);
%plot(eg,x);
%plot(p,x);
%plot(dl,x);
%plot(dg,x);
```